Research Article

Clostridioides difficile spore-entry into intestinal epithelial cells contributes to recurrence of the disease.

Pablo Castro-Córdova[1,2], Paola Mora-Uribe[1], Rodrigo Reyes-Ramírez[1,2], Glenda Cofré-Araneda[1], Josué Orozco-Aguilar[1,2], Christian Brito-Silva[1,2], María José Mendoza-León[1,2], Sarah A. Kuehne[3], Nigel P., Minton[4], Marjorie Pizarro-Guajardo[1,2,5] and Daniel Paredes-Sabja[1,2,5*].

[1]Microbiota-Host Interactions and Clostridia Research Group, Facultad de Ciencias de la Vida, Universidad Andrés Bello, Santiago, Chile.

[2]Millennium Nucleus in the Biology of Intestinal Microbiota, Santiago, Chile.

[3]School of Dentistry and Institute for Microbiology and Infection, University of Birmingham, Birmingham, UK.

[4] BBSRC/EPSRC Synthetic Biology Research Centre, School of Life Sciences, Centre for Biomolecular Sciences, The University of Nottingham, Nottingham, United Kingdom.

[5] Department of Biology, Texas A&M University, College Station, TX, 77843, USA.

Running Title: Internalization of *C. difficile* spores into IECs and effect in pathogenesis

Key Words: *C. difficile* spore, spore internalization, recurrent *C. difficile* infection, animal model.

***Corresponding author:**

Dr. Daniel Paredes-Sabja, Department of Biology, Texas A&M University, College Station, TX, 77843, USA. E-mail: dparedes-sabja@bio.tamu.edu

Abstract

Clostridioides difficile spores produced during infection are essential for the recurrence of the disease. However, how *C. difficile* spores persist in the intestinal mucosa to cause recurrent infection remains unknown. Here, we show that *C. difficile* spores gain entry into the intestinal mucosa via fibronectin-$\alpha_5\beta_1$ and vitronectin-$\alpha_v\beta_1$ specific-pathways. The spore-surface exosporium BclA3 protein is essential for both spore-entry pathways into intestinal epithelial cells. Furthermore, *C. difficile* spores of a *bclA3* isogenic mutant exhibited reduced entry into the intestinal mucosa and reduced recurrence of the disease in a mouse model of the disease. Inhibition of *C. difficile* spore-entry led to reduced spore-entry into the intestinal epithelial barrier and recurrence of *C. difficile* infection *in vivo*. These findings suggest that *C. difficile* spore-entry into the intestinal barrier is a novel mechanism of spore-persistence that can contribute to infection recurrence and have implications for the rational design of therapies.

Introduction.

Clostridioides difficile is a strict anaerobic Gram-positive pathogenic bacterium that forms highly resistant spores that easily persist in the environment and contribute to transmission of *C. difficile* infections (CDI) through fecal-oral route[1]. Disruption of the gut microbiota by the use of broad-spectrum antibiotics leads to an optimal environment for *C. difficile* colonization and proliferation in the colon and disease manifestation. CDI currently leads hospital-acquired diarrhea associated to antibiotics in United States and world-wide[2]. In the US alone, ~500,000 patients per year become infected with CDI, and mortality rates reach ~8% of total patients[2]. The annual cost of CDI to the health care system is estimated in ~US 4.8 billion[2]. Treatment of CDI usually involves antibiotic therapy, typically vancomycin or metronidazole and, most recently, fidaxomicin[2], which, although resolves the infection in ~95% of the cases, leads to recurrence of CDI (R-CDI) in 15-30% of the individuals[3-5].

During infection, *C. difficile* produces two major virulence factors, toxins TcdA and TcdB, which are responsible for the clinical manifestation of the disease, induce pro-inflammatory cytokines, disruption of tight junctions, detachment of intestinal epithelial cells (IEC) and loss of trans-epithelial barrier[6]. *C. difficile* also initiates a sporulation pathway that leads to the production of new metabolically dormant spores in the host's intestine[1]. *In vivo*, spore-formation is essential for the recurrence of the disease[7]. Moreover, spore-based therapies that remove *C. difficile* spores from the intestinal mucosa contribute to reduce recurrence of the disease in animal models[8].

Recent *in vivo* studies in the laboratory strain 630 suggest that the spore surface mucus-binding protein, peroxiredoxin-chitinase CotE, and the exosporium collagen-like BclA1 proteins are required for the colonization and infectivity in a mouse model of CDI[9,10]. However, the surface layer of 630 spores does not resemble that of clinically relevant strains which exhibit hair-like projections in their spore surface; structures that are absent in strain 630[1,11,12]. Importantly, most clinically relevant sequenced *C. difficile* isolates, including isolates of the epidemically relevant 027 ribotype, have a truncated *bclA1* due to a premature stop codon in the N-terminal domain[13], resulting in the translation of a small polypeptide, which localizes to the spore surface[10]; thus limiting the breadth and depth of these results.

C. difficile spores exhibit high levels of adherence to intestinal epithelial cells (IECs) *in vitro*[14,15], and that the hair-like projections of *C. difficile* spores come in close proximity with the microvilli of differentiated Caco-2 cells; furthermore, *C. difficile* spores interact in a dose-dependent manner with fibronectin (Fn) and vitronectin (Vn)[15], two extracellular matrix proteins used by several enteric pathogens to infect the host[16,17]. However, the mechanisms that underline how these interactions contribute to *C. difficile* spore-persistence *in vivo* and contribute to the recurrence of the disease remain unclear.

Herein we first demonstrate that *C. difficile* spores gain entry into the intestinal epithelial barrier of mice and that spore-entry into IECs requires serum-molecules, specifically Fn and Vn, that are luminary accessible in the colonic mucosa. We also demonstrate that the spore-entry pathway into IECs is Fn-$\alpha_5\beta_1$ and Vn-$\alpha_v\beta_1$. Next, we demonstrate that the spore surface collagen-like BclA3 protein is essential for spore-entry

into IECs through these pathways *in vitro* and essential for spore adherence to the intestinal mucosa. Importantly, BclA3 contributes to the recurrence of the disease in mice. We also observed the therapeutic potential of blocking spore-entry into the intestinal epithelial barrier and how co-administration of nystatin with vancomycin reduces spore-persistence and R-CDI in mice. Together, our results reveal a novel mechanism employed by *C. difficile* spores that contributes to R-CDI, which involves gaining intracellular access into the intestinal barrier via BclA3-Fn-$\alpha_5\beta_1$ and BclA3-Vn-$\alpha_v\beta_1$ specific, and that blocking spore-entry contributes to reduced recurrence of the disease.

Results

***C. difficile* spores internalize into the intestinal barrier *in vivo*.** To study the interaction of *C. difficile* spores and the host's intestinal barrier, we used a colonic/ileal loop assay infected with *C. difficile* spores for 5 hours[18], where *C. difficile* R20291 spores, were labeled with anti-spore antibodies[13,18]. We observed similar levels of adherence of *C. difficile* spores to the colonic and ileum mucosa (Fig. 1 a–c), with no preference for the site of spore-adherence in both colonic and ileum mucosa (Fig. 1d, Extended Data Fig. 1 and 2). Strikingly, we observed that *C. difficile* spores were able to cross the mucosal barrier in the colonic/ileal loop assay (Fig. 1a, b, e, f, Supplementary Video 1 and 2 and Extended Data Fig. 3, and 4). We observed that 4.6 and 3.7 spores per 10^5 μm^{-2} were able to cross the mucosal barrier in colonic and ileal loops (Fig. 1e), corresponding to 0.92% ± 0.30% and 1.04%±0.48 of the total spores, respectively. In the colonic mucosa internalized *C. difficile* spores were found to homogeneously localize 10 to 30 μm from the colonic surface and 5 to 50 μm from the closest crypt membrane, while in the ileum mucosa spores were

112 homogeneously found at 15 to 70 µm from the villus tip and 10 to 50 µm from the villus
113 membrane in ileal loops, (Extended Data Fig. 5), indicating multiple sites of entry in colon
114 and ileum.
115
116 ***C. difficile* spore-entry into intestinal epithelial cells requires serum components *in***
117 ***vitro*.**
118 Our previous *in vitro* studies in IECs were conducted in the absence of fetal bovine serum
119 (FBS) and did not evidence internalized spores[14,15,18,19]. Therefore, we assess if FBS
120 contributed to spore-entry by confocal fluorescence microscopy by analyzing monolayers
121 of polarized T84 IECs (Fig. 2a and Extended Data Fig. 6a, b) and differentiated Caco-2
122 cells (Extended Data Fig. 6c, d) which were infected with *C. difficile* spores of the
123 epidemically relevant R20291 and the commonly used strain 630 in the presence of FBS. In
124 both cell lines, several intracellular spores of strain *C. difficile* 630 were found to be located
125 between the apical and basal actin cytoskeleton (Fig. 2a and Extended Data Fig 6). To
126 obtain convincing evidence of entry of *C. difficile* spores into IECs, we analyzed polarized
127 monolayers of T84 and Caco-2 cell lines infected with *C. difficile* 630 or R20291 spores
128 using transmission electron microscopy (TEM). Electron micrographs evidence that some
129 *C. difficile* spores were found extracellularly in the apical membrane, while others were
130 found intracellularly (Fig. 2b–d). Intracellular *C. difficile* spores were surrounded by an
131 endosomal-like membrane (Fig. 2c, d). Notably, the formation of membrane lamellipodia-
132 like protrusions and circular ruffle surrounding *C. difficile* 630 spores were evidenced at the
133 site of attachment of *C. difficile* spores to the apical membrane (Fig. 2e), suggesting

macropinocytosis-like endocytosis of *C. difficile* spores. Intracellular spores of the strain, R20291, were also evidenced in differentiated Caco-2 cells (Fig. 2f–h).

Next, to quantitatively assess the internalization of *C. difficile* spores into non-phagocytic cells, we developed an exclusion assay in which, in non-permeabilized cells, only extracellular spores are fluorescently labeled with anti-*C. difficile* spore antibody, while total spores can be quantified by phase-contrast microscopy; intracellular spores are not stained by anti-*C. difficile* spore antibody (absence of fluorescence) and are only detectable by phase-contrast microscopy (Extended Data Fig. 7a). With this assay, we probed that entry of 630 and R20291 spores into monolayers of Caco-2, T84, Vero, and HT29 cell lines significantly increased in the presence of FBS (Fig. 2i, j), as well as with serum from various mammalian species (Fig. 2k). The percentage of internalized spores of 630 and R20291 strains was highest at 5 h post-infection in Caco-2 and T84 cells (Extended Data Fig. 7b, c). Spores of various clinically relevant ribotypes were able to internalize into Caco-2 cells (Extended Data Fig. 7d). Overall, these results demonstrate that *C. difficile* spores are able to gain intracellular entry into non-phagocytic cells and that spore-entry is serum-dependent *in vitro*.

***C. difficile* spore-entry into intestinal epithelial cells requires Fn and Vn.** Fn and Vn are extracellular matrix proteins, which are also present in mammal serum and are widely used by enteric pathogens to infect host cells[16,17]. We have shown previously that both, Fn and Vn, bind in a concentration-dependent manner to *C. difficile* spores[15]. To assess whether serum Fn and Vn contribute to *C. difficile* spore-entry, we evaluated the internalization assay in the presence of RGD peptide to block the interaction of Fn and Vn with their cognate receptors through the RGD binding domain[20,21]. RGD significantly reduced the

158 extent of spore-entry into differentiated Caco-2 cells in the presence of human serum by
159 ~45% (Figure 3a, Extended Data Fig. 8a), indicating that serum Fn and Vn might be
160 involved in *C. difficile* spore-entry in an RGD specific manner; by contrast, no decrease in
161 adherence of *C. difficile* spores was evidenced in the presence of RGD (Fig. 3b, Extended
162 Data Fig. 8b). Similar results were observed in undifferentiated Caco-2 cells (Extended
163 Data Fig. 8c–f). We confirmed these results by showing that the infection with spores pre-
164 incubated with Fn or Vn restored spore-entry into differentiated (Fig. 3c) and
165 undifferentiated Caco-2 cells (Extended Data Fig. 9a), but had no impact in spore-
166 adherence to differentiated (Fig. 3d) and undifferentiated Caco-2 cells (Extended Data Fig.
167 9b). Similar results were observed in differentiated Caco-2 cells pre-treated with Fn or Vn
168 before infection with *C. difficile* spores (Extended Data Fig. 9c, d), confirming that the
169 presence of Fn and Vn mediates *C. difficile* spore-entry.
170
171 **Intestinal barrier sites with accessible Fn and Vn.** Both Fn and Vn are mainly located in
172 the basal and basolateral membrane of epithelial cells where tight and adherent junctions
173 are formed[16,17]. However, several the epithelial barrier suffers reorganization and/or
174 disruption of tight and adherent junctions such as cell extrusion sites, goblet cells (GCs), at
175 cell-cell junctions with neighboring cells and along villus epithelial folds[22-24]. Therefore,
176 we hypothesized that sites undergoing adherent junction rearrangement also contained
177 accessible Fn and Vn. We performed double staining, in which luminally accessible Fn and
178 E-cadherin (Ecad), a marker for reorganization or disruption of adherent junctions[22], were
179 stained in non-permeabilized tissue. We first determined the relative number of IECs in the
180 colonic tissue that expresses luminally accessible Ecad and found that nearly 16% of the
181 IECs have this feature (Fig. 3h). Accessible Fn and Vn were observed in 27% and 14% of

the IECs cells (Fig. 3i and 3k). We observed that most of the cells that had luminally accessible Fn or Vn also had accessible Ecad (Fig. 3j, l), and are likely undergoing major reorganization of the adherent junctions. However, a small fraction of epithelial cells with accessible Fn (33%) or Vn (12%) had no accessible Ecad (Fig. 3i, k). Luminally accessible Ecad has been previously found around mucus-expelling GCs in mice intestinal tissue[22]. Therefore, to quantify the relative abundance of GCs with accessible Ecad in our experimental conditions, we performed double immunostaining for accessible Ecad and the GC-specific marker Muc2[22,25]. We observed that 13% of the IECs were positive for Muc2 in colonic tissue (Fig. 3m) and all of Muc2-positive cells were positive for accessible Ecad (Fig. 3n). Luminally accessible Ecad has also been observed in mice ileal tissue[22]; we observed that nearly 17% of the IECs of mice ileal had luminal accessible Ecad (Extended data Fig. 10a, b). Next we quantified the relative abundance of GCs in the ileum mucosa and observed that nearly 9% of total IECs were positive for Muc2 (Extended Data Fig. 10c), of which 70% were positives for accessible Ecad (Extended Data Fig. 10d). This data supports the notion that Fn and Vn are also accessible in the intestinal epithelial barrier. Altogether, these results demonstrate the existence of sites in the intestinal barrier that undergo reorganization of adherent junctions that exhibit accessible Fn and Vn through which *C. difficile* spores can gain entry into the intestinal barrier.

C. difficile spores internalize via Fn-$\alpha_5\beta_1$ and Vn-$\alpha_v\beta_1$ integrin _in vitro_. The Fn RGD loop between domains FnIII9 and FnIII10 enhances binding between Fn and $\alpha_5\beta_1$ integrin[16]; Vn also has a similar RGD loop that enhances binding to $\alpha_v\beta_1$ integrin[17]. To address whether binding of Fn and Vn to their cognate integrin receptors is required for *C.*

205 *difficile* spore-entry into IECs, monolayers of Caco-2 cells were infected with *C. difficile*
206 R20291 spores in the presence of the inhibitory RGD peptide, showing that in the presence
207 of Fn or Vn, increasing concentrations of RGD progressively decreased spore-entry into
208 differentiated (Fig. 4a, b) and into undifferentiated Caco-2 cells (Extended Data Fig. 11a,
209 c), but not spore-adherence (Fig. 4c, d, Extended Data Fig. 10b, d) to Caco-2 cells. Next,
210 through an antibody blocking assay, we assessed which integrin subunits are involved in
211 Fn- and Vn-dependent entry of *C. difficile* spores into IECs. Results demonstrate that
212 blocking the subunits of the collectin-binding, $\alpha_2\beta_1$ integrin[26,27] and β_3 integrin subunit did
213 not affect internalization nor adherence of *C. difficile* spores to Caco-2 cells in the presence
214 of Fn (Fig. 4e, f) or Vn (Fig. 4g, h). However, a significant decrease in spore-entry, but not
215 spore-adherence, to differentiated and undifferentiated Caco-2 cells was observed upon
216 blocking each subunit of $\alpha_5\beta_1$ integrin in the presence of Fn (Fig. 4e, f, Extended Data Fig.
217 11e, f), as well as blocking each subunit of $\alpha_v\beta_1$ integrin in the presence of Vn (Fig. 4g, h,
218 Extended Data Fig. 11g, h). These results were confirmed upon expressing each integrin
219 subunit in Chinese hamster ovary (CHO) cells (Fig. 4i–k), a naïve cell line that otherwise
220 does not express integrins. CHO cells expressing individual α_5 or β_1 integrin subunits
221 exhibited significant spore-entry but not adherence in the presence of Fn (Fig. 4l, m);
222 equally, CHO cells expressing individual α_v or β_1 integrin subunit exhibited significant
223 spore-entry but not spore-adherence in the presence of Vn (Fig. 4n, o). No increase in entry
224 or adherence was detected in the absence of Fn and Vn (Extended Data Fig. 12 a, b).
225 Altogether, these observations demonstrate that the internalization of *C. difficile* spores into
226 IECs occurs through Fn-$\alpha_5\beta_1$- and Vn-$\alpha_v\beta_1$ uptake pathways.
227

Fn and Vn bind to the hair-like extensions of *C. difficile* spores, formed by the collagen-like BclA3 exosporium protein. *C. difficile* spores of epidemically relevant strains exhibit hair-like projections that are likely to be formed by the collagen-like exosporium proteins[1,13]. Fn and Vn have a gelatin/collagen-binding domain[16,17], suggesting that these molecules might interact with *C. difficile* spores through these hair-like projections. Indeed, through TEM coupled with immunogold labeling of Fn and Vn, we observed that more than ~50% of the spores were positive for Fn- or Vn-immunogold particles (Extended Data Fig. 13a, b); immunogold Fn- and Vn-specific particles were observed in proximity to the hair-like extensions of *C. difficile* R20291 spores (Fig. 5a, b), suggesting that these structures might be implicated in spore-entry into IECs. Most epidemically relevant strains encode two collagen-like exosporium proteins, BclA2, and BclA3[1,13]. During the sporulation of R20291 strain, *bclA3* expression levels are ~60-fold higher than those of *bclA2*[28]. Consequently, we first hypothesized whether BclA3 was responsible for the formation of the hair-like extensions. Therefore, we constructed a single *bclA3* mutant strain, in an epidemic R20291 background, by removing the entire gene through a *pyrE*-based allelic exchange system[29] (Extended Data Fig. 14). Electron micrographs demonstrate that, as expected, wild-type R20291 (Δ*pyrE*/*pyrE*$^{+}$) spores exhibited typical hair-like projections observed in previous reports[1,11,12] (Fig. 5c). By contrast, the Δ*bclA3* deletion mutant formed spores that lacked the hair-like projections (Fig. 5d) that were restored upon complementation of the Δ*bclA3* mutant strain with a single wild-type copy of *bclA3* in the *pyrE* locus (Δ*bclA3*/*bclA3*$^{+}$; Fig. 5e), indicating that BclA3 is required for the formation of these projections on the surface of *C. difficile* spores.

BclA3 is required for Fn-$\alpha_5\beta_1$- and Vn-$\alpha_v\beta_1$-mediated spore-entry into IECs. To address whether BclA3 exosporium protein is implicated in *C. difficile* spore-entry into IECs, we first assayed whether the absence of BclA3 protein affected the internalization of *C. difficile* spores into IECs in the presence of Fn or Vn. As a control, we ensured that the anti-*C. difficile* spore goat serum used to quantify extracellular *C. difficile* spores, recognized Δ*bclA3* mutant spores (Extended Data Fig. 15a–c). Spores of the *C. difficile* Δ*bclA3* mutant strain exhibited a significant decrease in spore-entry into Caco-2 cells, but not adherence, to monolayers of Caco-2 cells was observed upon infection with *C. difficile* spores Δ*bclA3* mutant in the presence of Fn (Fig. 5f, g) and Vn (Fig. 5h, i). Importantly, the defect in spore-entry of the Δ*bclA3* mutant strain in the presence of Fn or Vn was restored to wild-type levels of internalization Δ*bclA3*/*bclA3*$^+$ strain (Fig. 5f–i), indicating that BclA3 is required for Fn- and Vn-mediated internalization into IECs. We further confirmed these results in monolayers of HeLa cells, evidencing essentially identical results (Extended Data Fig. 16 a–d). Next, to address whether Fn-$\alpha_5\beta_1$ and Vn-$\alpha_v\beta_1$-mediated spore-entry is BclA3-specific, we carried out infection experiments with Δ*bclA3* mutant spores in monolayers of CHO cells expressing individual integrin subunits. In the presence of Fn, a significant decrease in spore-entry (Fig. 5j, k), but not in adherence (Extended Data Fig. 16e, f), was observed upon infection of CHO cells expressing the α_5 or β_1 integrin subunit with Δ*bclA3* mutant spores. Similarly, Δ*bclA3* mutant spores internalized to a significantly lesser extent than wild-type spores during infection of CHO cells expressing α_v or β_1 integrin receptors in the presence of Vn (Fig. 5l, m); however, the absence of BclA3 had no impact on spore-adherence to CHO cells in the presence of Vn (Extended Data Fig. 16g, h). Fn- and Vn-mediated internalization of *C. difficile* spores into CHO cells expressing each

integrin subunit was restored to wild-type levels upon infection with spores Δ*bclA3*/*bclA3*$^{+}$ (Fig. 5j–m). Collectively, these results demonstrate that BclA3-Fn-$\alpha_5\beta_1$- and BclA3-Vn-$\alpha_v\beta_1$ are two pathways through which *C. difficile* spores can internalize into non-phagocytic cells.

Inactivation of the exosporium protein BclA3 decreases spore-adherence, but not spore-entry, of *C. difficile* spores to the intestinal mucosa. To assess whether the collagen-like BclA3 exosporium protein also contributed to the internalization of *C. difficile* spores into the intestinal mucosa *in vivo*, we used a colonic and ileal loop mouse model (Fig. 6a-c, Extended data Fig. 17 a-c). In contrast to our *in vitro* data, analysis of colonic mucosa sections show that inactivation of *bclA3* leads to a significant decrease of ~60% in spore-adherence per 10^5 μm^2 to the ileum mucosa (Fig. 6d); however, no differences were observed in spore internalization relative to the total adhered-spores (Fig. 6e). A similar trend was evidenced in ileal loops, where Δ*bclA3* spores adhered in a ~50% lower than wild-type spores per 10^5 μm^2 (Fig. 6f); however, no differences were observed in spore internalization relative to total adhered-spores (Fig. 6g). The defects in spore-adherence to the colonic and ileum mucosa were restored to wild-type levels upon complementing the wild-type *bclA3* allele in the Δ*bclA3* mutant (Fig. 6d–g, Extended data Fig. 17 a-c). Strikingly, these data indicate that the collagen-like BclA3 exosporium protein is required for *C. difficile* spore adherence to the intestinal mucosa, and that additional spore-surface proteins are contributing to redundant spore-entry pathways *in vivo*.

The *C. difficile* collagen-like BclA3 exosporium protein contributes to spore-persistence and recurrence of the disease in mice. Since BclA3 is essential for spore-entry into IECs *in vitro* and for adherence in the intestinal mucosa *in vivo*, we hypothesized that BclA3 might mediate spore-persistence and contribute to R-CDI. Therefore, antibiotic-treated mice were infected with spores of wild-type (Δ*pyrE*/*pyrE*$^{+}$), Δ*bclA3* and Δ*bclA3*/*bclA3*$^{+}$ strains (Fig. 6h). All three groups of mice exhibited similar weight loss during the initiation of CDI, and all manifested signs of diarrhea within 3 days post-infection (Extended Data Fig. 17d, e). Similar levels of *C. difficile* spores shed in feces were observed during the initiation of CDI between mice infected with wild-type (Δ*pyrE*/*pyrE*$^{+}$), and the mutants Δ*bclA3* and Δ*bclA3*/*bclA3*$^{+}$ (Extended Data Fig. 17f). These results indicate that the absence of BclA3 does not affect the initiation of CDI. Next, the impact of BclA3 in the recurrence of the infection was assessed by treating *C. difficile* infected mice with vancomycin for 5 days (Fig. 6h), R-CDI was monitored from day 8 post-infection. No significant differences in weight loss were evidenced after vancomycin treatment (days 8-11; Fig. 6i). However, a significant delay in the onset of diarrhea during R-CDI was observed after vancomycin treatment in mice infected with Δ*bclA3* mutant spores compared to wild-type infected-mice (Fig. 6j). The defect in R-CDI observed in Δ*bclA3* mutant infected-mice was restored to wild-type levels with the complemented Δ*bclA3/bclA3*+ strain (Fig. 6j). Although there were no significant differences in the levels of *C. difficile* spores, shed in the feces during R-CDI (Extended Data Fig. 17f), significantly lower CFUs of Δ*bclA3* mutant spores were detected in the medium colon compared to wild-type spores (Fig. 6k) but not in other sections of the intestinal tract (Extended Data Fig. 17g–i). Again, this defect was reverted in the complemented

319 Δ*bclA3/bclA3*+ strain (Fig. 6k). Cytotoxicity levels in the cecum content of Δ*bclA3* mutant-
320 infected mice were similar to those found in animals infected with wild-type strain
321 (Extended Data Fig. 17j). Collectively, these results demonstrate that the collagen-like
322 BclA3 exosporium protein is involved in *C. difficile* persistence and recurrence of the
323 disease.
324
325 **Inhibition of spore-entry into IECs renders *C. difficile* spores susceptible to**
326 **taurocholate-germination**. Since *C. difficile* spore-entry into IECs requires integrin
327 receptors, we tested whether cholesterol-lipid rafts, commonly required by integrin
328 receptors for endocytosis[30,31], were also required for uptake of *C. difficile* by IECs.
329 Therefore, we used the cholesterol-chelating agent, nystatin, which is a caveolin-related
330 pathway inhibitor that disrupts membrane microdomains known to be implicated in
331 integrin-mediated endocytosis and pathogen uptake[30,32]. Cells were preincubated with
332 nystatin for 1 h at 37 °C and infected in the same medium containing the inhibitor and *C.*
333 *difficile* spores. *C. difficile* spore-entry was inhibited in a dose-dependent manner into
334 Caco-2 cells and T84 cells (Fig 7a, b, Extended Data Fig. 18a, b). 30μM of nystatin
335 inhibited the spore-entry by about 80% in human cell lines Caco-2 and about 65% in T84
336 cells. We determined cell viability in the presence of nystatin by MTT at the highest
337 concentration of the inhibitor. Cell viability was generally around 90% (Extended Data Fig.
338 18c). These results suggest that *C. difficile* spore-entry is sensitive to cholesterol-
339 sequestering compounds.
340 Vancomycin administration leads to increased fecal-concentration of primary bile
341 acids[33] leading to enhanced *C. difficile* spore germination[34,35], suggesting that luminal

342 taurocholate would trigger germination of extracellular *C. difficile* spores that could
343 subsequent become inactivated by vancomycin. Therefore, we hypothesize that intracellular
344 spores should remain dormant in the presence of taurocholate. To test this hypothesis,
345 monolayers of 1-h nystatin-treated or untreated Caco-2 cells were infected for 3h with
346 serum-treated *C. difficile* spores. Next, infected monolayers were washed and treated with
347 taurocholate to trigger germination of extracellular spores, followed by ethanol-treatment to
348 inactivate germinated *C. difficile* spores. We observed that not all of the spores became
349 ethanol-sensitive upon taurocholate-treatment of infected Caco-2 monolayers (Fig. 7c),
350 suggesting that internalized spores were protected from taurocholate-triggered germination.
351 We confirmed this by evidencing a significant increase in ethanol-sensitive germinated
352 spores in the presence of nystatin (Fig. 7c). These results indicate that blocking *C. difficile*
353 spore-entry contributes to taurocholate-triggered germination of *C. difficile* spores and
354 subsequent spore-inactivation.
355
356 **Inhibition of *C. difficile* spore-entry into the intestinal barrier reduces recurrence of**
357 **the disease in mice.** To address whether *in vivo C. difficile* spore-entry into the intestinal
358 barrier also required RGD-binding integrins[36], colonic and ileal loop assays were assessed
359 in the presence of RGD during *C. difficile* spore infection (Fig. 7d, e, Extended data Fig
360 18d, e). Ileal and colonic loops were injected with RGD peptide and *C. difficile* spores
361 during 5h, then were processed and visualized in confocal microscopy. Consistent with our
362 *in vitro* data, in the colonic loop sections, we observed that presence of RGD peptide
363 reduced spore internalization by ~82% (Fig. 7g), while no difference in spore-adherence
364 was observed (Fig. 7h); similarly, in ileal loop sections, we observed that RGD peptide
365 decreased spore internalization by ~90% (Fig. 7i) and does not affect the spore adherence

366 to the ileum mucosa (Fig. 7j). These results demonstrate that *C. difficile* spore-entry *in vivo*
367 is RGD-binding integrin-dependent.

368 Since the RGD-dependency of spore-entry into the intestinal barrier is likely
369 attributed to integrin receptors, we address whether the cholesterol-sequestering drug,
370 nystatin, could block internalization of *C. difficile* spores into the intestinal barrier *in vivo* in
371 the colonic and ileum mouse mucosa. Mice were treated for 24-h with nystatin or saline as
372 a control prior to surgery and during intestinal loop-infection (Fig. 7d, f, Extended data Fig
373 18d, f) then were infected with *C. difficile* spores for 5h, then tissues were processed for
374 confocal microscopy. In the colonic loop section, we observed that nystatin had no effect
375 on spore internalization (Fig. 7g) and in spore-adherence to the colonic mucosa (Fig. 7h);
376 however, in the ileal loop sections, the presence of nystatin significantly decreased spore
377 internalization by ~96% (Fig. 7i), and no effect in *C. difficile* spore-adherence to the ileum
378 mucosa was observed (Fig. 7j).

379 Since *C. difficile* spore-entry prevents taurocholate-germination, contributing to the
380 persistence of *C. difficile* spores during the disease; we hypothesized that administration of
381 the inhibitor of spore-entry, nystatin, during CDI-treatment with vancomycin, could reduce
382 the recurrence of the infection in a previously developed mouse model of R-CDI[8] (Fig. 7k).
383 To address this question, antibiotic-treated mice were infected with *C. difficile* R20291
384 spores. During the first episode of CDI, both groups of mice had similar levels of weight
385 loss, the timing of the onset of diarrhea and shed similar amounts of *C. difficile* spores
386 during the initiation of CDI (days 1-3) (Extended Data Fig.18g–i). At day 3 post-infection,
387 animals were treated with vancomycin or a mixture of vancomycin and nystatin for 5 days
388 (Fig. 7k). Vancomycin-treated mice exhibited a significant decrease in weight during R-
389 CDI, which became highest at day 11 post-infection (4th day after vancomycin treatment;

Fig. 7k, m). By contrast, CDI-animals treated with vancomycin and nystatin had no significant decrease in weight loss during the recurrence of the infection (Fig. 7k, n). These observations were confirmed upon monitoring the onset of diarrhea during R-CDI (Fig. 7o), where we observed a significant delay in the onset of recurrent diarrhea in CDI-mice treated with the mixture of vancomycin and nystatin compared to vancomycin alone (Fig. 7o). The animals shed similar amounts of *C. difficile* spores during R-CDI (Extended Data Fig. 18i). Collectively, these results demonstrate that the administration of a pharmacological inhibitor of internalization of *C. difficile* spores during vancomycin treatment delays the incidence of recurrence of the infection.

Discussion

During CDI, *C. difficile* spore-formation is essential in the recurrence of the disease[7], yet the underlying mechanisms that correlate *C. difficile* spore-persistence and recurrence of the disease remain unclear. In this study, we unravel a novel and unexpected mechanism employed by *C. difficile* spores to interact with the intestinal mucosa that contributes to the recurrence of disease. Our results have identified host molecules, cellular receptors, and a spore-surface ligand involved in spore-entry into IECs. Importantly, intracellular spores remain dormant in the presence of germinant. Using nystatin, a pharmacological inhibitor of spore-entry in combination with antibiotic treatment, leads to a reduction in the recurrence of the disease in mice. Together, these observations open a new angle for therapeutic interventions of CDI to prevent the recurrence of the disease.

Our results identified host molecules and cellular receptors involved in the entry of *C. difficile* spores into IECs. The presence of Fn or Vn allows *C. difficile* spores to gain intracellular access to IECs, in an RGD-specific manner, and through specific integrin

414 receptors (i.e., $\alpha_5\beta_1$ and $\alpha_v\beta_1$). These observations were confirmed by the *in vivo* inhibition
415 of *C. difficile* spore-entry in the presence of the RGD peptide, which specifically inhibits
416 interactions between Fn-$\alpha_5\beta_1$ and Vn-$\alpha_v\beta_1$[20,21]. Although Fn and Vn are mainly located in
417 the basal and basolateral membrane of IECs contributing to cell polarity[16,17], antibody
418 staining of healthy ileum and colonic tissue demonstrate that Fn and Vn are luminally
419 accessible in a significant fraction of the IECs. Most of these cells were positive for
420 luminally accessible Ecad, and suggests that these cell types include cell-extrusion, cells
421 next to extrusion sites, and epithelial folds that typically undergo adherent junction
422 reorganization[22-24]. However, a small fraction of cells positive for luminally accessible Fn
423 and Vn were negative for luminally accessible Ecad, suggesting a novel phenotype within
424 cells at the intestinal epithelial barrier. We also confirmed previous observations in mice
425 that identified GCs have luminally accessible Ecad[22], suggesting that these cell types might
426 also be targeted by *C. difficile* spores to gain entry into the epithelial barrier. M cells are an
427 additional cell-type that might contribute to *C. difficile* spore-entry into the intestinal
428 epithelial barrier includes since they expresses β_1-integrin at the apical surface in contrast
429 to its normal basolateral location in enterocytes[22,37,38]. The fact that *in vivo* spore entry was
430 RGD-binding integrin-specific, suggests that Fn and Vn are accessible and employed by *C.*
431 *difficile* spores to gain entry into IECs, which is consistent with the presence of accessible
432 Fn and Vn in ileal and colonic loops. It is noteworthy that while RGD-specific entry was
433 observed in both ileal and colonic loops, nystatin was only able to reduce spore-entry into
434 the ileum, but not colonic mucosa. This suggests that caveolae-independent endocytosis of
435 *C. difficile* spores might prime in the colonic epithelia. During CDI, C. *difficile* toxins
436 disrupt adherent junctions, leading to progressive exposure of deep regions of the colonic

437 epithelium as infection advances. One consequence of this cellular disorganization may be
438 an alteration to the distribution of cell receptors that may lead to increased adherence and
439 internalization of *C. difficile* spores into the intestinal mucosa. Together, these observations
440 prompt further studies to address how epithelium remodeling contributes to persistence of
441 *C. difficile* spores and recurrence of the disease.

442 Another major contribution of this work is the role of the spore surface collagen-like
443 BclA3 exosporium protein in *C. difficile* spore-entry into IECs in a Fn-$\alpha_5\beta_1$- and Vn-$\alpha_v\beta_1$-
444 dependent manner. Our previous work shows that Fn and Vn bind in a dose-dependent
445 manner to *C. difficile* spores[15]. By immunogold-electron microscopy, our results
446 demonstrate that Fn and Vn bind to the hair-like projections of *C. difficile* spores. We also
447 demonstrate that they are formed by the collagen-like exosporium glycoprotein BclA3. It is
448 noteworthy that experiments with monolayers of Caco-2 cells and CHO cells expressing
449 integrin subunits demonstrate that BclA3 is essential for spore-entry in the presence of Fn
450 and Vn in a integrin-dependent manner; results that contrast with BclA3 being essential for
451 adherence to the intestinal mucosa, but not for spore-entry into the intestinal barrier.
452 Coupling these results with those of *in vivo* RGD-specific *C. difficile* spore-entry into the
453 intestinal barrier, indicates that additional spore-surface proteins might play redundant roles
454 during *in vivo* spore-entry. Regardless of these incongruencies, we observed that BclA3
455 contributes to the recurrence of the disease in a mouse model, suggesting that BclA3-
456 mediated spore-adherence to the intestinal mucosa might contribute to spore persistence
457 and recurrence of the disease. The differences in spore-adherence to the colonic tissue after
458 R-CDI observed in the medium colonic tissue of mice might relate to the absence of
459 mucosal folds typically observed in the distal and proximal colon of mice[39]. Here, we have

460 shown that BclA3 uses Fn and Vn and their specific integrins to gain-entry into IECs and
461 that BclA3 is essential for *C. difficile* spore adherence to the intestinal mucosa and
462 contributes to the recurrence of the disease.

463 The work presented here also shows that *C. difficile* spore-entry into IECs
464 contributes to spore dormancy in the presence of primary bile salts (i.e., taurocholate), and
465 that blocking *in vivo* spore-entry during antibiotic treatment (vancomycin), leads to reduced
466 recurrence of CDI in mice. This brings a broader understanding of how strict anaerobic
467 spore-formers can persist in the host and remain dormant in a dysbiosis environment
468 enriched with bile acids that trigger spore germination. Intracellular bacterial spores may
469 survive until released back to the luminal environment to recolonize the host. Although the
470 precise mechanism of how intracellular spores would contribute to the recurrence of the
471 disease is unclear and prompts further studies, it may involve the rapid renewal of the
472 intestinal epithelium, which, due to rapid proliferation and differentiation of multipotential
473 stem cells located in the crypts of Lieberkühn[40-43], renew the epithelial barrier every 5 days.
474 The factors that contribute to infection recurrence, although partly linked to continued
475 disruption of the microbiota[44], are also directly linked to the persistence of *C. difficile*
476 spores in the host. This is particularly relevant for CDI, considering that the rates for
477 recurrent CDI are around ~18 to 32%, and may rise between 45 and 65% during subsequent
478 recurrent episodes[2,44]. Importantly, this *C. difficile* spore-entry phenotype provides an
479 additional point of intervention of disease recurrence and therapeutic susceptibility. The
480 cholesterol-sequestering drug, nystatin, is FDA approved for oral administration[45], raising
481 new approaches to develop pharmacological formulations that target *C. difficile* spore-entry

482 during disease. Similarly, BclA3 and $\alpha_5\beta_1$ and $\alpha_v\beta_1$ integrins are also candidates drug

483 targets to combat recurrent *C. difficile* infections.

484

485 **Methods.**

486 **Data reporting.** No statistical methods were used to predetermine the sample size. The
487 experiments were not randomized, and investigators were not blinded to allocation during
488 experiments and outcome assessment.

489

490 **Bacterial strains and growth conditions.** *C. difficile* strains (See Table S1) were
491 routinely grown at 37 °C under anaerobic conditions in a Bactron III-2 anaerobic chamber
492 (Shellab, USA) in BHIS medium: 3.7% weight vol^{-1} brain heart infusion broth (BD, USA)
493 supplemented with 0.5% weight vol^{-1} yeast extract (BD, USA) and 0.1% weight vol^{-1} L-
494 cysteine (Merck, USA) or on BHIS agar plates. *E. coli* strains were routinely grown
495 aerobically at 37 °C under aerobic conditions with shaking (200 r.p.m.) in Luria-Bertani
496 (LB) medium (BD, USA), supplemented with 25 μg mL^{-1} chloramphenicol (Merck, USA),
497 where appropriate.

498 For mutant construction, a defined *C. difficile* minimal medium (CDMM) media
499 was prepared as described by Cartman and Minton[46] as an uracil-free medium when
500 performing genetic selections. For CDMM broth preparation, 5× amino acids (50 mg mL^{-1}
501 casamino acids, 2.5 mg mL^{-1} L-tryptophan, 2.5 mg mL^{-1} L-cysteine), 10× salts (50 mg
502 mL^{-1} Na_2HPO_4, 50 mg mL^{-1} $NaHCO_3$, 9 mg mL^{-1} KH_2PO_4, 9 mg mL^{-1} NaCl), 20× glucose
503 (200 mg mL^{-1} D-glucose), 50× trace salts (2.0 mg mL^{-1} $(NH_4)_2SO_4$, 1.3 mg mL^{-1}
504 $CaCl_2 \cdot 2H_2O$, 1.0 mg mL^{-1} $MgCl_2 \cdot 6H_2O$, 0.5 mg mL^{-1} $MnCl_2 \cdot 4H_2O$, 0.05 mg mL^{-1}
505 $CoCl_2 \cdot 6H_2O$), 100× iron (0.4 mg mL^{-1} $FeSO_4 \cdot 7H_2O$) and 100× vitamins (0.1 mg mL^{-1} D-
506 biotin 0.1, mg mL^{-1} calcium-D-pantothenate, 0.1 mg mL^{-1} pyridoxine) stock solutions were
507 made by dissolving their components in Milli-Q water and filter sterilizing (0.2-μm pore

size) prior to use. Solutions were mixed to obtain a final CDMM media made of 10 mg mL^{-1} casamino acids, 0.5 mg mL^{-1} L-tryptophan, 0.5 mg mL^{-1} L-cysteine, 5 mg mL^{-1} Na_2HPO_4, 5 mg mL^{-1} $NaHCO_3$, 0.9 mg mL^{-1} KH_2PO_4, 0.9 mg mL^{-1} NaCl, 10 mg mL^{-1} D-glucose, 0.04 mg mL^{-1} $(NH_4)_2SO_4$, 0.026 mg mL^{-1} $CaCl_2{\cdot}2H_2O$, 0.02 mg mL^{-1} $MgCl_2{\cdot}6H_2O$, 0.01 mg mL^{-1} $MnCl_2{\cdot}4H_2O$, 0.001 mg mL^{-1} $CoCl_2{\cdot}6H_2O$, 0.004 mg mL^{-1} $FeSO_4{\cdot}7H_2O$, 0.001 mg mL^{-1} D-biotin, 0.001 mg mL^{-1} calcium-D-pantothenate and 0.001 mg mL^{-1} pyridoxine[46]. For solid medium, agar (BD, USA) were mixed with CDMM to a final concentration of 1.0% weight vol^{-1}. Finally, media were supplemented with uracil (Sigma–Aldrich, USA) at 5 mg mL^{-1} and 5-Fluoroorotic acid (5-FOA) (USBiological USA) at 2 mg mL^{-1} as described[47,48].

Cell Lines and Reagents. Caco-2, Vero, HT29, and Chinese hamster ovary (CHO) were obtained from ATCC (USA). Dr. Mauricio Farfán (Universidad de Chile, Chile) gently provided T84 cells. Caco-2 and Vero were routinely grown at 37 °C with 5% of CO_2 with Dulbecco's modified Eagle's minimal essential medium (DMEM) High Glucose (HyClone, USA); CHO cells in Ham's F-12K (Kaighn's) medium; T84 in DMEM/F12 1:1 (HyClone, USA); and HT29 in RPMI 1640. All media were supplemented with 10% vol vol^{-1} inactivated Fetal Bovine Serum (FBS) (HyClone, USA) and 100 U ml^{-1} penicillin, and 100 µg ml^{-1} streptomycin (HyClone, USA). T84 cells were cultured onto Transwell (Corning USA) until 1,000–2,000 Ω. For transfected CHO cells (CHO-α_v, CHO-α_5, and, CHO-β_1), the culture media was supplemented with 1,500 µg mL^{-1} geneticin (HyClone USA). For immunofluorescence experiments, cells were plated over glass coverslip in a 24-wells plate and cultured for 2-days post confluence (undifferentiated) or 8-days post-confluence (differentiated), changing the culture medium every other day.

Spore Preparation. Spores preparation was done as previously has been published[18]. Briefly, 100 µL of 1:1,000 dilution of an overnight culture in BHIS was plated in 70:30 agar plates that were prepared as follow: 6.3% weight vol^{-1} (BD, USA), 0.35% weight vol^{-1} protease peptone (BD, USA), 0.07% ammonium sulfate $(NH_4)_2SO_4$ (Merck USA), 0.106% weight vol^{-1} Tris base (Omnipur, Germany), 1.11% weight vol^{-1} brain heart infusion extract (BD, USA) and 0.15% weight vol^{-1} yeast extract (BD, USA), 1.5% weight vol^{-1} Bacto agar (BD, USA). Plates were incubated for 7 days at 37 °C under anaerobic conditions in anaerobic chamber Bactron III-2 (Shellab USA). Then plates were removed from the chamber, and colonies were scraped out with ice-cold sterile Milli-Q water. Then the sporulated culture was washed five times with ice-cold Milli-Q water in micro-centrifuge at 18,400×*g* for 5 min each. To separate spores, the sporulated culture was loaded in 45% weight vol^{-1} autoclaved Nycodenz (Axell USA) solution and centrifugated at 18,400×*g* for 40 min. Spore pellet was separated and washed 5 times at 18,400×*g* for 5 min with ice-cold sterile Milli-Q water to remove Nycodenz. Spores were counted in Neubauer chamber, and volume adjusts at 5×10^9 spores mL^{-1} and stored at −80 °C.

***C. difficile* mutant construction by allelic exchange.** Primer design and amplification of *C. difficile* R20291 strain were based on the available *C. difficile* genomes from the EMBL/GenBank databases with accession number FN545816. The oligonucleotides and the plasmids/strains used in this study are listed in Table S1 and Table S2, respectively. In-frame deletions in *C. difficile* R20291 were made by allelic exchange using *pyrE* alleles[47].

554 To remove the *bclA3* gene, a 1086 bp allelic exchange cassette was obtained by
555 overlap extension PCR of the LHA and RHA originated by amplification with primer pairs
556 P332 (FP-LHA-bclA3-pyrE)/P334 (RP-LHA-bclA3-pyrE) and P335 (FP-RHA-bclA3-
557 pyrE)/P336 (RP-RHA-bclA3-pyrE), each of 544 bp and 542 bp in size. The resulting
558 cassette yielded complete removal of the entire *bclA3* cassette. Next, this cassette was
559 cloned into Sbf1/AscI sites in pMTL-YN4, giving plasmid pDP376. To verify the correct
560 construction of the plasmids, all constructs were Sanger sequenced.
561 The plasmids obtained were transformed into *E. coli* CA434 (RP4) and mated with
562 *C. difficile* R20291 Δ*pyrE*[47]. *C. difficile* transconjugants were selected by sub-culturing on
563 BHIS agar containing 15 µg mL^{-1} thiamphenicol (Sigma–Aldrich USA) and 25 µg mL^{-1}
564 cefoxitin (Sigma–Aldrich USA) and re-streaked five times. The single-crossover mutants
565 identified were streaked onto *C. difficile* minimal medium (CDMM) [49] with 1.5% weight
566 vol^{-1} agar supplemented with 2 mg mL^{-1} 5-Fluoroorotic acid (USBiological, USA) and 5
567 µg mL^{-1} uracil (Sigma–Aldrich USA) in order to select for plasmid excision. Confirmation
568 of plasmid excision was made by negative selection in BHIS-thiamphenicol plates. The
569 isolated FOA-resistant and thiamphenicol resistant colonies were screened using the primer
570 pair P664 (FP-bclA3-detect) / P665 (RP-bclA3-detect) for the *bclA3* mutant. All mutants
571 were whole-genome sequenced to confirm the genetic background and that no additional
572 SNPs were introduced during the genetic manipulation. For correction of the *pyrE*
573 mutation, transconjugants with pMTL-YN2C were streaked onto minimal media without
574 uracil or FOA supplementation, and developed colonies were analyzed further.
575
576 **Complementation by allelic exchange at the *pyrE* locus**. To complement the Δ*bclA3*
577 mutation, a 3,564 bp fragment containing 372 bp upstream of the start codon of *bclA3* and

the entire bicistronic operon formed by *sgtA* and *bclA3* was PCR amplified with primer pairs P476 (NFP-bclA3c-promotor)/P477 (NRP-bclA3c) and cloned into BamHI/EcoRI sites of pMTL-YN2C, giving plasmid pMPG1. Next, plasmid pMPG1 was transformed into *E. coli* CA434 and subsequently conjugated with *C. difficile* R20291Δ*pyrE* Δ*bclA3*, respectively, as described above. The transconjugants obtained were streaked onto CDMM and tested by colony PCR using primer pair P530 (Fp-*pyrE* detect)/P529 (RP-*pyrE* detect) for *pyrE* reversion. Complemented strains were also subjected for whole-genome sequencing.

Transfections of CHO cells with α_5, α_v and, β_1 integrins. The integrins subunits were overexpressed in CHO cells line with the following plasmids: Alpha 5 integrin-GFP (Addgene plasmid# 15238)[50], miniSOG-Alpha-V-Integrin-25 (Addgene plasmid # 57763)[51] and Beta1-GFP in pHcgreen donated by Martin Humphries (Addgene plasmid # 69804)[52]. CHO cells were seeded on coverslips in 24-well plates until reach 70-90% of confluency and were transfected using Lipofectamine® LTX (Invitrogen USA) according to manufacturer protocol with 1 µg of each plasmid. Transfected cells were analyzed and confirmed by positive GFP fluorescence in epifluorescence microscopy. When the population GFP positive cells were higher than 50%, were selected for geneticin resistance with 1,500 µg mL^{-1} of geneticin until ~100% of GFP positive cells, and the level of expression of the integrin subunits in the cells was confirmed by Western blot.

SDS-PAGE and Western blot of transfected CHO cells. Transfected CHO cells were washed and homogenized with RIPA buffer that was prepared as follow: 50 mM buffer Tris HCl (Omnipur, Germany); 150 mM NaCl (Sigma–Aldrich, USA); 0.5% weight vol^{-1}

602 deoxycholate (Sigma–Aldrich, USA); 1% vol vol^{-1} NP 40 (Sigma–Aldrich, USA); 1 mM
603 EGTA (Sigma–Aldrich, USA); 1 mM EDTA (Sigma–Aldrich); 0.1% weight vol^{-1} SDS
604 (Winkler, USA). The cell lysate was centrifuged at 18,400×*g* for 30 min at 4 °C, and
605 protein concentration was quantified by BCA protein kit (RayBiotech USA). Next, 20 µg of
606 protein were suspended in 2X SDS-PAGE sample loading buffer, boiled and
607 electrophoresed on 12% vol vol^{-1} and 4% vol vol^{-1} acrylamide SDS-PAGE gels (Bio-Rad
608 Laboratories, Canada) on MiniProtean® camera (Bio-Rad Laboratories, Canada). Then
609 proteins were transferred to a nitrocellulose membrane (Bio-Rad Laboratories, Canada).
610 Membranes were blocked then probed in Tris-Buffered saline containing 0.1% vol vol^{-1}
611 Tween (TTBS), with 2% weight vol^{-1} BSA, incubated with mouse anti-α_v, α_5 and β_1
612 antibody (SC166665, SC376156 y SC374429; Santa Cruz Biotechnologies, USA) and
613 1:1,000 mouse anti-alpha tubulin (T5168 Sigma–Aldrich USA) in 2% BSA-TTBS as
614 loading control at concentration and were washed 3 times with TTBS. Membranes were
615 incubated with 1:10,000 vol vol^{-1} secondary antibody anti-mouse horseradish peroxidase
616 (HRP) conjugate (A5278, Sigma–Aldrich, USA) in 2% weight vol^{-1} BSA-TTBS. HRP
617 activity was detected with a chemiluminescence detection system (Fotodyne Imaging
618 system, USA.) by using PicoMax sensitive chemiluminescence HRP substrate (Rockland
619 Immunochemicals, USA.).
620
621 **Germination assay of extracellular *C. difficile* spores in Caco-2 cells.** Two–day old
622 confluent monolayers of Caco-2 cells were treated with 30 µM of nystatin for 1 h at 37 °C
623 or DMEM high glucose without FBS as control. To infect cells, *C. difficile* spores at an
624 MOI of 10 were pre-incubated 1 h at 37 °C with 20 µL of NHS and then suspended in 200
625 µL that were added to each well; FBS final concentration 10% vol vol^{-1}.

To remove unbound spores, monolayers were washed 3 times with PBS, and cells were incubated with 0.1% weight vol^{-1} sodium taurocholate (Sigma–Aldrich, USA) in DMEM for 1 h at 37 °C (or DMEM as control) and washed 3 times with PBS. Cells were treated with 100% ethanol for 10 min, and cells were lysed with PBS-0.06% Triton X-100 for 10 min, plated in BHIS-CC supplemented with 0.1% weight vol^{-1} sodium taurocholate and incubated at 37 °C overnight. The number of CFU mL^{-1} was determined, and the percentage of adherence relative to the control.

Infection of monolayers of cell lines with *C. difficile* spores. Adherence and intracellular spores were examined using a differential immunofluorescence staining procedure, as previously described[14,53] with modifications. To evaluate the dynamic of *C. difficile* spore in Caco-2 cells and T84 cells. Caco-2 and T84 cells were grown on coverslips in 24–wells tissue culture plates until they reach a monolayer of 2-days post-confluency and were infected for 0.5, 1, 3, 5, and 8 h at 37 °C at an MOI of 10 of *C. difficile* spores pre-incubated 1h at 37 °C with 20µL of FBS and then suspended in the infection volume of 200µL that was added to each well. Then were washed gently in PBS prior to immunostaining as described below.

To evaluate if *C. difficile* internalize in different cell lines, undifferentiated, differentiated Caco-2, T84, Vero and HT29 cells were infected at 37 °C with an MOI 10 with *C. difficile* spore strain 630, and R20291 preincubated 1h at 37 °C with FBS or DMEM as control as was described above. Were washed gently in PBS prior to immunostaining, as described below.

Also, undifferentiated Caco-2 cells were infected at an MOI of 10 with *C. difficile* spores preincubated 1h at 37 °C with FBS, mouse serum (Pacific Immunology, USA), rat

650 serum (Pacific Immunology, USA), rabbit serum (Pacific Immunology, USA) and NHS
651 (Complement Technology USA) as was described above. Then were washed gently in PBS
652 prior to immunostaining, as described below.

653 To evaluate if *C. difficile* internalization occurs in different strains, undifferentiated
654 Caco-2 cells were infected at an MOI of 10 with *C. difficile* spores R20291, M120 and
655 spores of *C. difficile* clinical isolates PUC52, PUC30, PUC 25, PUC31, PUC 98 and PUC
656 131[54], which were pre-incubated 1h at 37 °C with FBS as was described above. Then were
657 washed gently in PBS prior to immunostaining, as described below.

658 To assess that the internalization of *C. difficile* spores into IECs is through the
659 specific interaction between Fn or Vn and their cognate integrin receptors, infection
660 experiments were done in the presence of the RGD peptide [20,21]. Briefly, differentiated and
661 undifferentiated Caco-2 cells were incubated with 0, 1, 3, and 5 µg mL^{-1} of RGD peptide
662 (Abcam USA) for 1 h, 37 °C then were infected for 3h at 37 °C with spores pre-incubated
663 1h at 37 °C with NHS as was described above, then samples were washed gently in PBS
664 prior to immunostaining as described below.

665 To evaluate whether the internalization of the spores is mediated by Fn and Vn,
666 differentiated and undifferentiated Caco-2 cells were treated for 1h 37 °C at with 10 µg
667 mL^{-1} of purified human Fn or human Vn in DMEM and then were infected with an MOI 10
668 of untreated *C. difficile* spores R20291. Also, the infection was performed using untreated
669 Caco-2 cells that were infected for 3h at 37 °C with an MOI 10 of *C. difficile* spores pre-
670 incubated for 1h at 37 °C with 10 µg mL^{-1} of human Fn or human Vn in DMEM. Then
671 samples were washed in PBS prior to the immunostaining as described below.

672 To confirm that the internalization of *C. difficile* spores is dependent of Fn and Vn,
673 we perform an infection assay in differentiated and undifferentiated Caco-2 cells that were

pre-incubated with 1, 3, or 5 µg mL^{-1} of RGD peptide and were infected with an MOI of 10 with *C. difficile* spores pre-incubated for 1h 37 °C with 10 µg mL^{-1} of purified human Fn or human Vn in DMEM. Then samples were washed in PBS prior to the immunostaining as described below.

To identify the integrin subunits implicated in spore-entry, an antibody blocking assay was performed using mouse monoclonal antibodies against individual integrin subunits: anti-human integrin α_5, α_v, (ab78614, ab16821; Abcam, USA), α_2, β_1 and β_3 (MAB1950Z, MAB1959Z, and MAB2023Z; Millipore USA); and control non-immune IgG antibody (I5006, Sigma–Aldrich, USA). Caco-2 cells were incubated with 200µL of DMEM with the appropriate antibodies at 5 µg mL^{-1} for 1 h at 37 °C. The cells were infected for 3h at 37 °C with spores pre-incubated for 1h at 37 °C with 10 µg mL^{-1} of purified human Fn or human Vn in DMEM. Then samples were washed in PBS prior to the immunostaining as described below.

In order to demonstrate that *C. difficile* spore entry requires the integrins subunits α_5, $\alpha_{v,}$ and $\beta_{1,}$ Then CHO cells with ectopic expression of α_5, α_v and, β_1 integrins, were infected 3 h at 37 °C with an MOI of 10 of *C. difficile* spores that were preincubated with 10 µg mL^{-1} of purified human Fn or human Vn in DMEM. Then samples were washed in PBS prior to the immunostaining as described below.

To evaluate whether the collagen-like exosporium protein BclA3 is required for *C. difficile* spore entry into intestinal epithelial cells is dependent of differentiated Caco-2 cells and monolayers of HeLa cells, were infected for 3 h at 37 °C with an MOI of 10 with wild-type (Δ*pyrE*/*pyrE*$^+$), Δ*bclA3* and Δ*bclA3*/*bclA3*+ *C. difficile* R20291 spores that were preincubated for 1h at 37 °C with 10 µg mL^{-1} of purified human Fn or human Vn in

DMEM. Then samples were washed in PBS prior to the immunostaining as described below.

To evaluate the effect of nystatin in the internalization of *C. difficile* spores, Caco-2 cells were pre-incubated with 6, 12, 18, 24, and 30 μM nystatin or T84 cells were incubated with 30μM of nystatin (Sigma–Aldrich USA) for 1 h at 37 °C in DMEM and in the same media were infected for 3 h at 37 °C with spores at an MOI 10 pre-incubated with FBS as was described above. At the used concentration of nystatin, the cell viability of treated Caco-2 cells and T84 for 4 h was ~90%, as was observed by trypan blue (Invitrogen USA) and MTT assay (Life Technologies USA) according to manufacturer protocols.

Immunofluorescence of adhered *C. difficile* spores in infected monolayers and epifluorescence analysis. The aforementioned infected monolayers of cells were subsequently fixed with PBS–4% paraformaldehyde for 10 min, then were washed 3 times and blocked with PBS–1% BSA overnight at 4 °C; in nonpermeabilized monolayers, the extracellular spores were marked with 1:50 anti–*C. difficile* spore goat serum (recognize specifically to *C. difficile* spores in infections of IECs infection assays) in PBS–1% BSA 1 h RT and 1:400 anti-goat conjugated with CFL 488 secondary antibody (green) (SC362255, Santa Cruz Biotechnologies, USA) in PBS–1% BSA for 1 h RT. The samples were washed three times with PBS and once with sterile distilled water. Samples were then dried at RT for 30 min, and coverslips were mounted using Dako Fluorescence Mounting Medium (Dako, Denmark) and sealed with nail polish. Samples were observed on an Olympus BX53 fluorescence microscope with UPLFLN 100× oil objective (numerical aperture 1.30). Images were captured with the microscope camera for fluorescence imaging

720 Qimaging R6 Retiga and pictures were analyzed with ImageJ (NIH, USA). Extracellular
721 spores or adhered were considerate as spores in phase contrast that were marked in
722 fluorescence. Internalized spores were considered as spores visible in phase contrast, but
723 that does not have fluorescence. A total of ~300 spores were analyzed per experimental
724 condition.
725
726 **Mice used.** 6-8 weeks C57BL/6 (male or female) were obtained from the breeding colony
727 at the Biological Science Department of Andrés Bello University derived from Jackson
728 Laboratories. Mice were housed with ad libitum access to food and water. Bedding and
729 cages were autoclaved, and mice had a 12-hour cycle of light and darkness. All procedures
730 were performed following the approved protocols by the Institutional Animal Care and Use
731 Committee of the Universidad Andrés Bello.
732
733 **Colonic and ileal loop assay.** C57BL/6 mice were anesthetized in an isoflurane chamber
734 (RWD USA) with 4% vol vol^{-1} isoflurane (Baxter USA) at and were maintained with 2%
735 vol vol^{-1} during the surgery administrated by air. The intestinal loop model was performed
736 as previously described[18]. Briefly, a midline laparotomy was performed, making 1–cm
737 incision in the abdomen, 1.5 cm ileal, and proximal colon (at 1.0 – 1.5 cm from the cecum
738 as a reference) were ligated with silk surgical suture. To evaluate the effect of NYS or RGD
739 peptide in *C. difficile* spore internalization, mice were treated with 17,000 UI kg^{-1} NYS (n
740 = 4) 24h before the surgery. In the loop, as control, mice were treated with 0.9% NaCl
741 (saline) (n = 4) then, ligated loops were injected with 3×10^8 *C. difficile* R20291. In the
742 case of RGD, ligated loops were injected with 250 nmol of RGD peptide (n = 4). To
743 evaluate the role of BclA3 protein in *C. difficile* spore internalization, the ligated loops

were injected with 100 µL of 0.9% weight vol^{-1} NaCl containing 5×10^8 wild-type spore (Δ*pyrE*/*pyrE*+) (SI *n* = 12; colon *n* = 10), Δ*bclA3* (SI *n* = 12; colon *n* = 12) and Δ*bclA3*/*bclA3*+ (SI *n* = 12; colon *n* = 11). The intestine was returned to the abdomen, and the incision was closed. Animals were allowed to regain consciousness. Mice were kept for 5 h and were euthanized. The ligated loops were removed and washed gently in PBS prior to immunostaining, as described below.

Immunostaining of ileal and colonic loops. First, extracted washed intestinal tissues from the ileal and colonic loops were longitudinally cut, then washed by immersion in PBS 3 times at room temperature (RT). For better visualization of the tissues, they were fixed flat at RT. To perform this, tissues were fixed over a filter paper imbibed with 30% sucrose (Winkler, Chile) in PBS–4% paraformaldehyde (Merck, USA) for at least 15 min. Tissues were transferred to a microcentrifuge tube with the same fixing solution and were incubated at 4 °C overnight. Since fixation of mucus with cross-linking agents, such as paraformaldehyde, cause mucus layer of colon to collapse and shrink to a very tiny lining the epithelia[55], we did not observe mucus layer in our ileal and colonic loops. Prior to immunostaining, the intestinal and colonic tissues were cut into ~5 × 5 mm fragments.

To quantify *C. difficile* spore adherence and internalization in the colonic and in the ileal mucosa, tissues were made permeable by incubation with PBS–0.2% Triton X-100 (Merck, USA) and blocked with PBS–3% BSA (Sigma–Aldrich, USA) for 3 h at RT, the same buffer was used for subsequent incubation with antibodies. Tissue was incubated with a primary polyclonal 1:1,000 anti-*C. difficile* spore IgY batch 7246 antibodies (Aveslab USA) in PBS–3% BSA that does not immunoreacted with epitopes of vegetative cells

767 neither with murine microbiota[8] and with 1:50 phalloidin Alexa-Fluor 568 (#ab176753
768 Abcam, USA) in PBS–3% BSA overnight at 4 °C to stain the actin cytoskeleton. Following
769 PBS washed, samples were incubated with 1:400 goat anti-chicken IgY secondary
770 antibodies Alexa-Fluor 488 (#ab150173 Abcam USA) in PBS–3% BSA at RT, washed 3
771 times with PBS and the cellular nuclei stained with 1:1,000 of Hoechst (ThermoFisher,
772 USA) for 15 min at RT.

773 To perform double immunostaining acc Fn, acc Vn, acc Muc2, with acc Ecad in
774 healthy colonic tissue or acc Muc2 with acc Ecad in the intestinal tissue, first the proximal
775 colon and ilium of 2 independent healthy C57BL/6 mice of 8 weeks old were removed, and
776 mice were sacrificed. Next, tissues were washed by immersion 3 times in PBS at RT and
777 they were fixed flat with 30% sucrose in PBS–4% paraformaldehyde as was described
778 above. Subsequently, tissued cut into ~5 × 5 mm fragments, then were blocked with PBS-
779 3% BSA (Sigma–Aldrich, USA) for 3 h at RT. And to immunostaining, the acc Ecad, 3
780 colonic and 1 intestinal tissue fragments of each mouse were incubated with a primary
781 polyclonal 1:200 rat anti-E-cadherin (#ab11512; Abcam USA) in PBS–3% BSA for
782 overnight at 4 °C, then tissues were washed, with PBS, and incubated with 1:300 goat anti-
783 rat IgG secondary antibodies Alexa-Fluor 488 (#A-21470, ThermoFisher, USA) in PBS–
784 3% BSA for 3 h at RT. Subsequently, to perform the second stain Fn, Vn or Muc2 in
785 tissues stained for accessible Ecad, all tissues fragments were washed with PBS and then
786 for i) stain accessible Fn one colonic tissue fragment of each mice was incubated with
787 1:200 of rabbit anti-fibronectin (SC9068, Santa Cruz Biotechnologies, USA), or to ii) stain
788 accessible Vn one colonic tissue fragment of each mice was incubated with 1:200 of rabbit
789 anti-vitronectin (SC15332, Santa Cruz Biotechnologies, USA), and finally iii) to stain

accessible Muc2 in colonic and ileum tissue one tissue fragment of each mice was incubated with 1:200 of rabbit anti-muc2 ab90007 Abcam (#ab90007. Abcam, USA), in PBS–3% BSA for overnight at 4 °C. at the next day, tissues were incubated with 1:300 of donkey anti-rabbit IgG secondary antibodies Alexa-Fluor 568 (A11036, Invitrogen, USA) for 3 h at RT. Subsequently, tissues were washed and were made permeable by incubation with PBS–0.2% Triton X-100 (Merck, USA) for 1 h at RT. Finally, tissues were incubated with 1:100 phalloidin Alexa-Fluor 647 (A22287 Invitrogen, USA) for 90 min at RT.

The aforementioned immune-stained tissues were subsequently mounted with the luminal side-up. For this, the colonic crypts and the intestinal villi were identified under light microscopy with 10× or 40× magnification and were oriented side-up towards the coverslip. The tissue segment was placed over 5µL of Dako fluorescent mounting medium (Dako, Denmark) applied onto a glass slide, and the tissue covered with 15 µL Dako fluorescent mounting medium and closed with a coverslip. Coverslips were affirmed to the glass slide with vinyl tape to hold the tissue sections in place and were allowed to cure for at least 24 h before imaging.

Confocal microscopic analysis of ileal and colonic loops. To acquiring images, two confocal fluorescent microscopes were used; a Leica TCS LSI and a Leica SP8 (Leica, Germany) at the Confocal Microscopy Core Facility of the Universidad Andrés Bello. In the fist instance to observe spore internalization in the healthy ileum and colonic mucosa, a Leica TCS LSI was used, with 63× ACS APO oil objective numerical aperture 1.3, and 5× (optical zoom 20×), numerical aperture 0.5. Confocal micrographs were acquired using excitation wavelengths of 405 nm, 488 nm, and 532 nm, and signals were detected with an

ultra-high dynamic PMT spectral detector (430–750 nm). Emitted fluorescence was split with four dichroic mirrors (QD405 nm, 488 nm 561 nm, and 635 nm). Images (1,024 × 1,024 pixels). To observe the sites with acc Fn and Vn in the intestinal barrier and to evaluate the adherence and internalization of the Δ*bclA3* spore mutant to the intestinal barrier or to evaluate spore adherence and internalization in mice treated with RGD and NYS confocal images were acquired in Leica SP8 was used with HPL APO CS2 40× oil, numerical aperture 1.30. Signals, 3 PMT spectral detector PMT1 (410-483) DAPI PMT2 (505-550) Alexa-Fluor 488 PMT3 (587-726) Alexa-Fluor 555. Emitted fluorescence was split with dichroic mirrors DD488/552. Three-dimensional reconstructions of intestinal epithelium were performed using ImageJ software (NIH, USA). Villi and crypts were visualized by Hoechst and phalloidin signals. 3D reconstruction videos were performed with Leica software LASX 3D (Leica, Germany).

To quantify cells of the colonic and ileum mucosa with accessible proteins immunodetected, confocal images with a 1–µm Z step size were filtered with Gaussian Blur 3D (sigma x: 0.6; y: 0.6; z:0.6) and quantifies with cell counting plug-in of ImageJ 1,000 - 1,200 cells were counted in an area 84,628µm^2 per mice.

To quantify spore adherence and internalization, confocal images with a 0.7–µm Z step size were analyzed. Adhered spores were considered as fluorescent-spots that were in narrow contact with the actin cytoskeleton (visualized with phalloidin), and internalized spores were considered as fluorescent-spots that were inside the actin cytoskeleton in the three spatial planes (orthogonal view)[23,56]. The analyzed area for each tissue was 338,512 µm^2 per animal.

Then we evaluated the spore distribution of adhered and internalized in the colonic and in the intestinal mucosa. To measure the distribution of adhered spores in the colonic and ileum mucosa, the perpendicular distance from the center of the spore to the epithelium was measured using ImageJ (NHI, USA). In the case of internalized spores, we measured the perpendicular distance from the center of the spore to the mucosa surface or from the closest crypt membrane. For ileum mucosa, we measure the perpendicular distance from the center of the spore to the villus tip or to the villus membrane.

Visualization of spore internalization in intestinal epithelial cells *in vitro* by confocal microscopy. Differentiated Caco-2 cells, and T84 cells cultured onto Transwell (Corning USA) until 1,000–2,000 Ω. Cells were infected for 5 h with an MOI of 10 with *C. difficile* spores previously stained with Alexa Fluor 488 Protein Labeling Kit (Molecular Probes, USA) according to the manufacturer's instruction. Cells were washed 2 twice with PBS and were permeabilized with PBS–0.06%-Triton X-100 (Merck, USA) for 10 min at RT, were washed and incubated with 1:150 phalloidin Alexa-Fluor 568 (#ab176753 Abcam, USA) in PBS–1% BSA for 1h at RT. Then cells were washed, fixed and visualized in a confocal microscopy Olympus FV1000 of the Confocal Microscopy Core Facility of the Andrés Bello University.

Sample preparation for Transmission Electron Microscopy and Immuno-electron microscopy. To visualize internalized spores in IECs, six-well plates containing differentiated Caco-2 cells or T84 cells cultured in transwell as was described above were infected for 5 h at 37 °C at an MOI of 20 with *C. difficile* R20291 spores pre-incubated 1h at 37 °C with 100 µL of NHS (Complement Technology USA) for each well, and then was

suspended in the infection volume of 1mL; FBS final concentration 10% vol vol^{-1} FBS. Unbound spores rinsed o□, and cells were scraped, fixed, and processed, as is described below.

To evaluate the binding of Fn and Vn to the surface of *C. difficile* spores, 4×10^7 *C. difficile* spore- were incubated in PBS–0.2% BSA containing 10 µg ml^{-1} of human Fn and Vn for 1h at 37 °C. The spores were then washed three times (18,400×*g* for 5 minutes at RT) with PBS. Then the spores were pelleted by one cycle of centrifugation at 18,400 × *g* for 10 min. Pellets were then resuspended in 200 µl PBS-1% BSA, incubated for 30 min at RT, and then sedimented by centrifugation at 18,400 × *g* for 10 min at RT. Pellets were resuspended as above and incubated with primary antibody 1:200 rabbit pAb against Fn (SC9068, Santa Cruz Biotechnology USA) or Vn (SC15332, Santa Cruz Biotechnology, USA) in PBS-BSA 1% for 1 h at RT. The excess of antibody was eliminated by three cycles of centrifugation at 18,400×*g* for 5 min at RT and resuspension in PBS–0.1% BSA. Spore suspensions were then incubated for 1 h with 1:20 donkey anti-rabbit IgG antibody coupled to 12–nm gold particles (Abcam ab105295, USA) in PBS-1% BSA for 1h at RT. And were washed by triple centrifugation at 18,400×*g* for 5 min. Subsequently, samples were fixed and processed, as is described below.

To visualizes if the collagen-like BclA3 exosporium protein forms the hair like-extension of *C. difficile* spores, ~2×10^8 *C. difficile* purified spores of wild-type R20291 (Δ*pyrE*/*pyrE*$^+$), Δ*bclA3* and Δ*bclA3*/*bclA3*$^+$ fixed and processes as is described here below.

Sample processing and staining for transmission electron microscopy. The aforementioned spore or monolayers of infected IECs samples were fixed with freshly

prepared with 2.5% glutaraldehyde 1% paraformaldehyde in 0.1 M cacodylate buffer (pH 7.2) overnight at 4 °C, rinsed in cacodylate buffer, and stained for 30 min with 1% tannic acid. Then samples were serially dehydrated with acetone 30% (with or without 2% uranyl acetate) for 20 min, 50% for 20 min, 75% for 20 min, 90% for 20 min, and twice with 100% for 20 min, embedded in spurs resin at ratio acetone: spurs of 3:1, 1:1, and 1:3 for 40 min each and then resuspended in spurs for 4 h and baked overnight at 65 °C, and prepared for transmission electron microscopy as previously described[15]. Thin sections (90 nm) obtained with a microtome were placed on glow discharge carbon-coated grids for negative staining and double lead stained with 2% uranyl acetate and lead citrate. Grids were analyzed with a Phillips Tecnai 12 Bio Twin electron microscope of the Universidad Católica de Chile.

R-CDI mouse model. Antibiotic cocktail (ATB cocktail) was administrated, as was previously described [8]. Briefly, an antibiotic cocktail containing 40 mg kg^{-1} kanamycin (Sigma–Aldrich, USA), 3.5 mg $kg^{-}1$ gentamicin (Sigma–Aldrich, USA), 4.2 mg kg^{-1} colistin (Sigma–Aldrich, USA), 21.5 mg $kg^{-}1$ metronidazole (Sigma–Aldrich, USA) and 4.5 mg $kg^{-}1$ vancomycin (VAN) (Sigma–Aldrich, USA) was administrated via gavage for 3 days (days -6 to -4 before the infection). Then 1 day before the infection (day -1), an intraperitoneal (i.p.) injection of 10 mg kg^{-1} clindamycin (Sigma–Aldrich, USA) was administrated to all mice. The next day all mice were infected via gavage with 1×10^7 spores R20291, and on day 3 post-infection, DPBS containing 17,000 UI kg^{-1} of nystatin and 50 mg kg^{-1} vancomycin or vancomycin alone (as control) was orally administered for 5 days to 18 and 23 mice, respectively.

To evaluate the role of the exosporium protein BclA3 in the R-CDI, 40 treated mice with antibiotic cocktail followed with clindamycin, were infected orally with 100 µl PBS containing 5×10^7 *C. difficil*e spore strain R20291 of wild-type (Δ*pyrE*/*pyrE*+) (*n* = 10), Δ*bclA3* (*n* = 16) or Δ*bclA3*/*bclA3*+ (*n* = 14) strains. *C. difficile*-infected mice were housed individually in sterile cages with *ad libitum* access to food and water. All procedures and mouse handling were performed aseptically in a biosafety cabinet to contain spore mediated transmission and cross-contamination. Mice were daily monitored for loss weight, aspect, and diarrhea were measured to determine the endpoint of each animal.

During the entire experiment, the clinical condition (sickness behaviors and fecal samples) of mice was monitored daily with a scoring system. The presence of diarrhea was classified according to severity as follows: (i) normal stool (score = 1); (ii) color change and/or consistency (score = 2); (iii) presence of wet tail or mucosa (score = 3); (iv) liquid stools (score = 4). A score higher than 1 was considered as diarrhea[57]. At the end of the assay, animals were sacrificed with a lethal dose of ketamine and xylazine. Cecum content and colonic tissues were collected.

Quantification of *C. difficile* spores from feces and colon of mice. To quantify *C. difficile* spores in feces, daily collected fecal samples were stored at −20 °C until spore quantification.

Feces were hydrated in 500 µL sterile Milli-Q water overnight at 4 °C and then mixed with 500 µL of absolute ethanol (Merck, USA) for 60 min at RT. Then, serially dilutions of the sample were plated onto selective medium supplemented with 0.1% weight vol^{-1} taurocholate, 16 µg ml^{-1} cefoxitin, 250 µg mL^{-1} L-cycloserine and 1.5% weight vol^{-1} (BD,

928 USA) (TCCFA plates). The plates were incubated anaerobically at 37 °C for 48 h, colonies
929 counted, and results expressed as the Log_{10} (CFU g^{-1} of feces)[58]. Colonic tissue collected at
930 the end of the experiment was washed three times with PBS. The tissue *C. difficile* spore-
931 load was determined in the proximal colon, medium colon, distal colon, and cecum tissue.
932 Tissues were weighed and adjusted at a concentration of 100 mg mL^{-1} with a 1:1 mix of
933 PBS: absolute ethanol, then homogenized and incubated for 1 h at RT. The amounts of
934 viable spores were quantified plating the homogenized tissue onto TCCFA plates, as
935 described previously[18]. The plates were incubated anaerobically at for 48 h at 37 °C.
936 Finally, the colony count was expressed as the Log_{10} (CFU g^{-1} of the tissue).
937
938 **Cecum content cytotoxicity assay in Vero cells of infected mice during R-CDI.** Vero
939 cell cytotoxicity was performed as described previously[59]. At first, 96-well flat-bottom
940 microtiter plates were seeded with Vero cells at a density of 10^5 cells $well^{-1}$. Mice cecum
941 contents were suspended in PBS at a ratio of 1:10 (100 mg mL^{-1} of cecum content),
942 vortexed and centrifuged at 18,400×*g* for 5 min, the supernatant was sterilized with a
943 0.22µm filter and serially diluted in DMEM supplemented with 10% vol vol^{-1} FBS and 100
944 U ml^{-1} penicillin, and 100 µg ml^{-1} streptomycin; then 100 µL of each dilution was added to
945 wells containing Vero cells. Plates were screened for cell rounding 16 h after incubation at
946 37 °C. The cytotoxic titer was defined as the reciprocal of the highest dilution that
947 produced rounding in at least 80% of Vero cells per gram of luminal samples under 20×
948 magnification.
949

Statistical analysis. Prism 7 (GraphPad Software, Inc.) was used for statistical analysis. Student's *t*-test and the nonparametric test was used for pairwise comparison. Significance between groups was done by Mann-Whitney unpaired *t*-test. Comparative study between groups for *in vitro* experiments was analyzed by analysis of variance with post-hoc Student *t*-tests with Bonferroni corrections for multiple comparisons, as appropriate. A *P*-value of $\leq$ 0.05 was accepted as the level of statistical significance. Differences in the percentages of mice with normal stools, as well as percentages of mice with *C. difficile* infection, were determined by Gehan-Breslow-Wilcoxon test.

Acknowledgments

This work was funded by FONDECYT Regular 1191601 and FONDECYT Regular 1151025 to D.P-S. Millennium Nucleus of the Biology of the Intestinal Microbiota to D.P-S. PC-C had been supported by ANID doctoral fellowship 21161395 (Chile) and JO-A by OAICE-91-2018 of Universidad de Costa Rica. The authors acknowledge Rosario Hernandez-Armengol for technical assistance and Miriam Barros for useful discussion on image processing at the Confocal Microscopy Core Facility of the Universidad Andrés Bello. We certify that funding sources had no implication in the study design, collection of data, analysis, and interpretation of data.

Competing of Interests: DP-S and PC-C are inventors on a PCT patent relating to a method and pharmacological composition for the prevention of recurrent infections caused by *Clostridium difficile*, submitted by Universidad Andrés Bello. The other authors declare no competing interests.

References

1 Paredes-Sabja, D., Shen, A. & Sorg, J. A. *Clostridium difficile* spore biology: sporulation, germination, and spore structural proteins. *Trends Microbiol* **22**, 406-416.

2 Lessa, F. C. *et al.* Burden of *Clostridium difficile* infection in the United States. *N Engl J Med* **372**, 825-834.

3 Evans, M. E., Simbartl, L. A., Kralovic, S. M., Jain, R. & Roselle, G. A. *Clostridium difficile* infections in Veterans Health Administration acute care facilities. *Infect Control Hosp Epidemiol* **35**, 1037-1042.

4 Bakken, T. L. & Sageng, H. Mental Health Nursing of Adults With Intellectual Disabilities and Mental Illness: A Review of Empirical Studies 1994-2013. *Arch Psychiatr Nurs* **30**, 286-291.

5 Bouza, E. Consequences of *Clostridium difficile* infection: understanding the healthcare burden. *Clin Microbiol Infect* **18 Suppl 6**, 5-12.

6 Smits, W. K., Lyras, D., Lacy, D. B., Wilcox, M. H. & Kuijper, E. J. *Clostridium difficile* infection. *Nat Rev Dis Primers* **2**, 16020.

7 Deakin, L. J. *et al.* The *Clostridium difficile* spo0A gene is a persistence and transmission factor. *Infect Immun* **80**, 2704-2711.

8 Pizarro-Guajardo, M., Diaz-Gonzalez, F., Alvarez-Lobos, M. & Paredes-Sabja, D. Characterization of Chicken IgY Specific to *Clostridium difficile* R20291 Spores and the Effect of Oral Administration in Mouse Models of Initiation and Recurrent Disease. *Front Cell Infect Microbiol* **7**, 365.

9 Hong, H. A. *et al.* The Spore Coat Protein CotE Facilitates Host Colonization by *Clostridium difficile*. *J Infect Dis* **216**, 1452-1459.

10 Phetcharaburanin, J. *et al.* The spore-associated protein BclA1 affects the susceptibility of animals to colonization and infection by *Clostridium difficile*. *Mol Microbiol* **92**, 1025-1038.

11 Pizarro-Guajardo, M., Calderon-Romero, P., Castro-Cordova, P., Mora-Uribe, P. & Paredes-Sabja, D. Ultrastructural Variability of the Exosporium Layer of *Clostridium difficile* Spores. *Appl Environ Microbiol* **82**, 2202-2209.

12 Pizarro-Guajardo, M., Calderon-Romero, P. & Paredes-Sabja, D. Ultrastructure Variability of the Exosporium Layer of *Clostridium difficile* Spores from Sporulating Cultures and Biofilms. *Appl Environ Microbiol* **82**, 5892-5898.

13 Pizarro-Guajardo, M. *et al.* Characterization of the collagen-like exosporium protein, BclA1, of *Clostridium difficile* spores. *Anaerobe* **25**, 18-30.

14 Paredes-Sabja, D. & Sarker, M. R. Adherence of *Clostridium difficile* spores to Caco-2 cells in culture. *J Med Microbiol* **61**, 1208-1218.

15 Mora-Uribe, P. *et al.* Characterization of the Adherence of *Clostridium difficile* Spores: The Integrity of the Outermost Layer Affects Adherence Properties of Spores of the Epidemic Strain R20291 to Components of the Intestinal Mucosa. *Front Cell Infect Microbiol* **6**, 99.

16 Henderson, B., Nair, S., Pallas, J. & Williams, M. A. Fibronectin: a multidomain host adhesin targeted by bacterial fibronectin-binding proteins. *FEMS Microbiol Rev* **35**, 147-200.

17 Singh, B., Su, Y. C. & Riesbeck, K. Vitronectin in bacterial pathogenesis: a host protein used in complement escape and cellular invasion. *Mol Microbiol* **78**, 545-560.

18 Calderon-Romero, P. *et al.* *Clostridium difficile* exosporium cysteine-rich proteins are essential for the morphogenesis of the exosporium layer, spore resistance, and affect *C. difficile* pathogenesis. *PLoS Pathog* **14**, e1007199.

19 Barra-Carrasco, J. *et al.* The *Clostridium difficile* exosporium cysteine (CdeC)-rich protein is required for exosporium morphogenesis and coat assembly. *J Bacteriol* **195**, 3863-3875.

20 Redick, S. D., Settles, D. L., Briscoe, G. & Erickson, H. P. Defining fibronectin's cell adhesion synergy site by site-directed mutagenesis. *J Cell Biol* **149**, 521-527.

21 Leroy-Dudal, J., Gagniere, H., Cossard, E., Carreiras, F. & Di Martino, P. Role of alphavbeta5 integrins and vitronectin in Pseudomonas aeruginosa PAK interaction with A549 respiratory cells. *Microbes Infect* **6**, 875-881.

22 Nikitas, G. *et al.* Transcytosis of *Listeria monocytogenes* across the intestinal barrier upon specific targeting of goblet cell accessible E-cadherin. *J Exp Med* **208**, 2263-2277.

23 Pentecost, M., Kumaran, J., Ghosh, P. & Amieva, M. R. *Listeria monocytogenes* internalin B activates junctional endocytosis to accelerate intestinal invasion. *PLoS Pathog* **6**, e1000900.

24 Pentecost, M., Otto, G., Theriot, J. A. & Amieva, M. R. *Listeria monocytogenes* invades the epithelial junctions at sites of cell extrusion. *PLoS Pathog* **2**, e3.

25 van Klinken, B. J. *et al.* Gastrointestinal expression and partial cDNA cloning of murine Muc2. *Am J Physiol* **276**, G115-124.

26 Humtsoe, J. O. *et al.* A streptococcal collagen-like protein interacts with the alpha2beta1 integrin and induces intracellular signaling. *J Biol Chem* **280**, 13848-13857.

27 Caswell, C. C. *et al.* Identification of the first prokaryotic collagen sequence motif that mediates binding to human collagen receptors, integrins alpha2beta1 and alpha11beta1. *J Biol Chem* **283**, 36168-36175.

28 Girinathan, B. P. *et al.* Effect of tcdR Mutation on Sporulation in the Epidemic *Clostridium difficile* Strain R20291. *mSphere* **2**.

29 Ehsaan, M., Kuehne, S. A. & Minton, N. P. *Clostridium difficile* Genome Editing Using *pyrE* Alleles. *Methods Mol Biol* **1476**, 35-52.

30 Hoffmann, C. *et al.* Caveolin limits membrane microdomain mobility and integrin-mediated uptake of fibronectin-binding pathogens. *J Cell Sci* **123**, 4280-4291.

31 Gianni, T., Gatta, V. & Campadelli-Fiume, G. {alpha}V{beta}3-integrin routes herpes simplex virus to an entry pathway dependent on cholesterol-rich lipid rafts and dynamin2. *Proc Natl Acad Sci U S A* **107**, 22260-22265.

32 Sui, Z. H. *et al.* Intracellular Trafficking Pathways of Edwardsiella tarda: From Clathrin- and Caveolin-Mediated Endocytosis to Endosome and Lysosome. *Front Cell Infect Microbiol* **7**, 400.

33 Vrieze, A. *et al.* Impact of oral vancomycin on gut microbiota, bile acid metabolism, and insulin sensitivity. *J Hepatol* **60**, 824-831.

34 Theriot, C. M., Bowman, A. A. & Young, V. B. Antibiotic-Induced Alterations of the Gut Microbiota Alter Secondary Bile Acid Production and Allow for

Clostridium difficile Spore Germination and Outgrowth in the Large Intestine. *mSphere* **1**.

35 Theriot, C. M. *et al.* Antibiotic-induced shifts in the mouse gut microbiome and metabolome increase susceptibility to Clostridium difficile infection. *Nat Commun* **5**, 3114.

36 Kapp, T. G. *et al.* A Comprehensive Evaluation of the Activity and Selectivity Profile of Ligands for RGD-binding Integrins. *Sci Rep* **7**, 39805.

37 Clark, M. A., Hirst, B. H. & Jepson, M. A. M-cell surface beta1 integrin expression and invasin-mediated targeting of Yersinia pseudotuberculosis to mouse Peyer's patch M cells. *Infect Immun* **66**, 1237-1243.

38 Hamzaoui, N., Kerneis, S., Caliot, E. & Pringault, E. Expression and distribution of beta1 integrins in in vitro-induced M cells: implications for Yersinia adhesion to Peyer's patch epithelium. *Cell Microbiol* **6**, 817-828.

39 Treuting, P. M., Dintzis, S. M. & Montine, K. S. *Comparative anatomy and histology. A mousse, rat and human atlas*. Second Edition edn, 552 (2018).

40 Clevers, H. The intestinal crypt, a prototype stem cell compartment. *Cell* **154**, 274-284.

41 Noah, T. K., Donahue, B. & Shroyer, N. F. Intestinal development and differentiation. *Exp Cell Res* **317**, 2702-2710.

42 Cheng, H. & Leblond, C. P. Origin, differentiation and renewal of the four main epithelial cell types in the mouse small intestine. V. Unitarian Theory of the origin of the four epithelial cell types. *Am J Anat* **141**, 537-561.

43 Barker, N. Adult intestinal stem cells: critical drivers of epithelial homeostasis and regeneration. *Nat Rev Mol Cell Biol* **15**, 19-33.

44 Kelly, C. P. Can we identify patients at high risk of recurrent *Clostridium difficile* infection? *Clin Microbiol Infect* **18 Suppl 6**, 21-27.

45 Mukherjee, P. K. *et al.* Topical gentian violet compared with nystatin oral suspension for the treatment of oropharyngeal candidiasis in HIV-1-infected participants. *AIDS* **31**, 81-88.

46 Cartman, S. T. & Minton, N. P. A mariner-based transposon system for in vivo random mutagenesis of Clostridium difficile. *Appl Environ Microbiol* **76**, 1103-1109.

47 Ng, Y. K. *et al.* Expanding the repertoire of gene tools for precise manipulation of the Clostridium difficile genome: allelic exchange using *pyrE* alleles. *PLoS One* **8**, e56051.

48 Ingle, P. *et al.* Generation of a fully erythromycin-sensitive strain of Clostridioides difficile using a novel CRISPR-Cas9 genome editing system. *Sci Rep* **9**, 8123.

49 Karasawa, T., Ikoma, S., Yamakawa, K. & Nakamura, S. A defined growth medium for *Clostridium difficile*. *Microbiology* **141 (Pt 2)**, 371-375.

50 Laukaitis, C. M., Webb, D. J., Donais, K. & Horwitz, A. F. Differential dynamics of alpha 5 integrin, paxillin, and alpha-actinin during formation and disassembly of adhesions in migrating cells. *J Cell Biol* **153**, 1427-1440.

51 Shu, X. *et al.* A genetically encoded tag for correlated light and electron microscopy of intact cells, tissues, and organisms. *PLoS Biol* **9**, e1001041.

52 Parsons, M., Messent, A. J., Humphries, J. D., Deakin, N. O. & Humphries, M. J. Quantification of integrin receptor agonism by fluorescence lifetime imaging. *J Cell Sci* **121**, 265-271.

53 Paredes-Sabja, D., Cofre-Araneda, G., Brito-Silva, C., Pizarro-Guajardo, M. & Sarker, M. R. *Clostridium difficile* spore-macrophage interactions: spore survival. *PLoS One* **7**, e43635.

54 Plaza-Garrido, A. *et al.* Outcome of relapsing *Clostridium difficile* infections do not correlate with virulence-, spore- and vegetative cell-associated phenotypes. *Anaerobe* **36**, 30-38.

55 Johansson, M. E., Larsson, J. M. & Hansson, G. C. The two mucus layers of colon are organized by the MUC2 mucin, whereas the outer layer is a legislator of host-microbial interactions. *Proc Natl Acad Sci U S A* **108 Suppl 1**, 4659-4665.

56 Lee, S. M. *et al.* Bacterial colonization factors control specificity and stability of the gut microbiota. *Nature* **501**, 426-429.

57 Warren, C. A. *et al.* Vancomycin treatment's association with delayed intestinal tissue injury, clostridial overgrowth, and recurrence of Clostridium difficile infection in mice. *Antimicrob Agents Chemother* **57**, 689-696.

58 Trindade, B. C. *et al.* Clostridium difficile-induced colitis in mice is independent of leukotrienes. *Anaerobe* **30**, 90-98.

59 Theriot, C. M. *et al.* Cefoperazone-treated mice as an experimental platform to assess differential virulence of Clostridium difficile strains. *Gut Microbes* **2**, 326-334.

Figure Legend

Fig. 1 | *C. difficile* adherence and internalization into intestinal barrier *in vivo*. a, b Confocal micrographs of fixed whole-mount of **a** colonic mucosa, and **b** ileum mucosa (SI) loop of C57BL/6 mice infected with 5×10^8 *C. difficile* R20291 spores for 5 h. *C. difficile* spores are shown in red, F-actin is shown in green and nuclei in blue (fluorophores colors were digitally reassigned for a better representation). **c,** Adherence of *C. difficile* spores to SI and colonic mice tissue. **d,** Distance of adhered spores from the villus tip or from the colonic epithelial apical surface. **e**, Quantification of internalized *C. difficile* spores in the SI and colon. **f**, Distance of internalized spores from the villus tip for the ileum or from the epithelium surface for the colon. Micrographs are representative of mice (n = 3). White arrow indicates internalized *C. difficile* spores, empty arrow indicates adhered *C. difficile* spore. Scale bar, 20 µm. Error bars indicate the mean ± S.E.M. Statistical analysis was performed by Mann-Whitney test, ns indicates non-significant differences, * $P < 0.0001$.

Fig. 2 | *C. difficile* spores are internalized by intestinal epithelial cells. a Confocal microscopy of an internalized *C. difficile* 630 spore in T84 cells. *C. difficile* spores are shown in red, F-actin is shown in green (fluorophores colors were digitally reassigned for a better representation). Yellow lines indicate an internalized spore. **b**−**e** TEM of differentiated T84 cell monolayers infected with *C. difficile* 630 spores. Black and white arrows denote extracellular and intracellular *C. difficile* spores, respectively. **c**, **d** are magnifications of black squares of **b**. **e** show an adhered *C. difficile* spore and an apical membrane extension of T84 cells surrounding *C. difficile* spores. **f**−**h** TEM of differentiated

monolayers of Caco-2 cells infected with *C. difficile* R20291 spores. White arrows in panel **f** indicate internalized *C. difficile* spores. **g**, **h** are magnifications of black boxes in panel **f**. Internalization of *C. difficile* spores **i** strain 630 and, **j** R20291 pre-incubated with FBS or culture media in Caco-2 undifferentiated (2 days), differentiated (8 days), T84, Vero, and HT29. **k**, Internalization of *C. difficile* spores pre-incubated with serum of different mammalian species in Caco-2 cells. Error bars indicate the mean ± S.E.M. Scale bars **a** 5 µm; **c**, **d**, 100 nm; **e,** 1 µm; **f,** 2 µm; **g**, 200nm; **h**, 500nm.

Fig. 3 | *C. difficile* spore internalization requires Fn and Vn which are luminally accessible in the intestinal barrier. a Internalization **b** and adherence of *C. difficile* spores pre-incubated with NHS in differentiated Caco-2 monolayers in the presence of 5 µg RGD peptide. **c**, **d** differentiated Caco-2 cells were infected with *C. difficile* spores pre-incubated with DMEM, NHS, 10, or 20 µg mL^{-1} Fn or Vn. Data shown in each panel are normalized to the control (0 µg mL^{-1} RGD or DMEM) and represent the mean of three independent experiments. **e**, **f**, **g** confocal micrographs of fixed whole-mount of the healthy colon of C57BL/6 mice for **e**, acc Fn; **f**, acc Vn; and **g**, acc Muc2 with acc Ecad. The main figure shown a 3D projection, below magnifications and a z-stack of representative cells with different immunostaining. **h** Shown the cell repartition of cell immunodetected for acc Ecad. **i** Shown the cell repartition of cells immunodetected for acc Fn. **j** Cell repartition of total acc Fn cells that were immunodetected for acc E-cad. **k** shown the cell repartition of cells immunodetected for acc Vn. **l** Cell repartition of total acc Vn cells that were immunodetected for acc E-cad. **m** shown the cell repartition of cells immunodetected for acc Muc2. **n** Cell repartition of total acc Muc2 cells that were immunodetected for acc E-

cad. Acc-FN, acc-VN and Muc2 is shown in green, Acc-Ecad is shown in red and F-actin in grey (fluorophores colors were digitally reassigned for a better representation). Scale bar, 20µm. Micrographs are representative of mice (n = 2). 1,000 - 1,200 cells were counted for each mouse in an area 84,628µm^2. Error bars indicate mean ± S.E.M. Statistical analysis was performed by Student's *t*-test, ns indicates non-significant differences, * $P < 0.05$ and ** $P < 0.001$. Scale bar, 20 µm.

Fig. 4 | *C. difficile* spore internalization via fibronectin-$\alpha_5\beta_1$ and vitronectin-$\alpha_v\beta_1$ integrins intestinal epithelial cells. *C. difficile* spore internalization in **a**−**d** differentiated Caco-2 cells incubated for 1 h with 1, 3, and 5 µg/mL of RGD peptide and infected with *C. difficile* spores pre-incubated for 1 h with **a, c,** 10 µg mL^{-1} Fn and **b, d,** 10 µg mL^{-1} Vn. **e**−**h** Differentiated Caco-2 monolayers were incubated for 1 h with 10 µg mL^{-1} of antibody against α_v, α_2, α_5, β_1, β_3, non-immune IgG antibody or without antibody. Then were infected with *C. difficile* spores R20291 pre-incubated with 10 µg mL^{-1} of **e**, **f**, Fn or **g**, **h**, Vn. **i**−**k,** show immunoblotting of cell lysates of CHO cells transfected with ectopic expression of **i** α_5 (~120 kDa); **j** α_v (~120 kDa); and **k** β_1 (~120 kDa) and alpha-tubulin as a loading control (50 kDa). *C. difficile* spore **l, n** internalization or **m, o** adherence in CHO cells ectopically expressing α_v, α_5, β_1 integrins, of spores pre-treated 1 h with **l**, **o** 10 µg mL^{-1} of Fn and **n, o,** 10 µg mL^{-1} of Vn. Data shown in each panel are normalized to the control (0 µg mL^{-1} RGD, DMEM, or IgG) and represent the mean of three independent experiments. Error bars indicate mean ± S.E.M. Statistical analysis was performed by Student's *t*-test, ns indicates non-significant differences, * $P < 0.05$ and ** $P < 0.001$.

Fig. 5 | The collagen-like exosporium protein BclA3 is required for spore-entry into intestinal epithelial cells via Fn-$\alpha_5\beta_1$ and Vn-$\alpha_v\beta_1$. **a**, **b** Immunogold of Fn and Vn binding to the hair-like extensions of *C. difficile* spores. *C. difficile* spores R20291 were incubated with 10 μg mL^{-1} Fn or Vn for 1 h. Samples were processed and visualized for TEM. White arrows indicate anti-Fn or -Vn rabbit antibody and anti–rabbit–gold 12 nm antibody complex. **ce** TEM of wild-type (Δ*pyrE*/*pyrE*$^+$), Δ*bclA3* and Δ*bclA3*/*bclA3*+ *C. difficile* R20291 spores. **f, h** Internalization and **g**, **i** adherence in differentiated Caco-2 cells of wild-type (Δ*pyrE*/*pyrE*$^+$), Δ*bclA3* and Δ*bclA3*/*bclA3*+ *C. difficile* R20291 spores pre-incubated with **f**, **g** 10 μg mL^{-1} Fn and **h, i** 10 μg mL^{-1} Vn. **j**, **l** internalization and **k**, **m** adherence in CHO cells ectopically expressing: **j** α_5; **k**, **m**; β_1 or **l** α_v infected with wild-type (Δ*pyrE*/*pyrE*$^+$), Δ*bclA3* and Δ*bclA3*/*bclA3*+ *C. difficile* R20291 spores pre-incubated with **j**, **k** 10 μg mL^{-1} Fn and **l, m** 10 μg mL^{-1} Vn. Data shows internalization and adherence normalized to wild-type spores and represented the mean of three independent experiments. Error bars indicate the mean ± S.E.M. Statistical analysis was performed by Student's *t*-test, ns indicates non-significant differences, * $P < 0.005$, ** $P < 0.0001$. **a**–**e**, Scale bar, 100 nm.

Fig. 6 | BclA3 is involved in *C. difficile* spore adherence to the intestinal mucosa and delays the onset of diarrhea during R-CDI.

Intestinal loops of approximately ~1.5 cm of the ileum and colon were injected with 5×10^8 *C. difficile* R20291 spores of strains wild-type (Δ*pyrE*/*pyrE*$^+$) (SI $n = 12$; colon $n = 10$), Δ*bclA3* (SI $n = 12$; colon $n = 12$) and Δ*bclA3*/*bclA3*$^+$ (SI $n = 12$; colon $n = 11$). **a**–**c** Representative confocal micrographs. *C. difficile* spores are shown in red, F-actin is shown

in green and nuclei in blue (fluorophores colors were digitally reassigned for a better representation). The white arrows indicate internalized *C. difficile* spores, empty arrows indicate adhered *C. difficile* spore. Quantification of the spots (spores) number per 10^5 µm^2 relatives to wild-type of **d** adhered or **e** internalized in the ileum, and **f** adhered or **g** internalized in the colonic mucosa. **h** Schematics of the experimental design. Mice were infected with 5×10^7 *C. difficile* spores strain R20291, wild-type (Δ*pyrE*/*pyrE*$^+$) (n = 10), Δ*bclA3* (n = 16) or Δ*bclA3*/*bclA3*$^+$ (n = 14) and were treated with vancomycin from day 3 to 7 and were monitored daily for **i,** relative weight during the R-CDI, **j** onset of diarrhea during the R-CDI. Spore adherence to the colonic tract was evaluated on day 11 to **k** medium colon.

Error bars indicate the mean ± S.E.M. Statistical analysis was performed by **d**–**g** Mann-Whitney test; **j** Log-rank (Mantel-Cox) test ns indicates non-significant differences; * $P <$ 0.05, ** $P < 0.001$.

Fig. 7 | Nystatin reduces *C. difficile* spore internalization and reduces the R-CDI rates. **a** Internalization and **b** adherence of undifferentiated Caco-2 cells were pre-treated with 6, 12, 18, 24, and 30 µM of nystatin for 1 h and subsequently infected with *C. difficile* spores R20291 pre-incubated for 1 h with FBS. **c** Colony-forming units of spores on BHIS-CC with 0.1% of sodium taurocholate of a lysate of undifferentiated Caco-2 were pre-treated with 30 µM of nystatin (shown as NYS) or DMEM alone as control and infected with *C. difficile* spores, washed, and then treated with sodium taurocholate and ethanol (shown as EtOH). The cells were lysed and plated, so only spores that remain dormant after treating the cells with taurocholate (dormant) germinate in the plates. The number of CFU mL^{-1}

was determined, and the percentage of adherence relative to the control. Loops of approximately ~1.5 cm of the ileum and colon of C57BL/6 were injected with 3×10^8 *C. difficile* R20291 with 250 nmol of RGD peptide (n = 4), or 17,000 UI kg^{-1} nystatin (n = 4) and saline (0.9% NaCl) as Ctrl (n = 4). **d**−**f** Representative confocal micrographs *C. difficile* spore is shown in red, F-actin is shown in green and nuclei in blue (fluorophores colors were digitally reassigned for a better representation). The white arrow indicates internalized *C. difficile* spores, empty arrow indicates adhered *C. difficile* spore. Quantification of spots number (spores) per 10^5 μm^2 of **g** internalized and **h** adhered spores in the ileum mucosa or **i** internalized and **j** adhered spores in the colonic mucosa in of C57BL/6. **k** Schematics of the experimental design of a mouse model of R-CDI. ATB cocktail treated C57BL/6 mice were infected with 6×10^7 R20291 spores. The CDI symptoms were treated from days 3 to 7 with the inhibitor of spore internalization, nystatin and vancomycin (shown as VAN+NYS) (n = 18) or vancomycin alone as control (shown as VAN) (n = 23) and were monitored daily for **l** relative weight during the R-CDI. Weight loss comparison for animals treated with **m** vancomycin or **n** vancomycin and nystatin and **o** onset to diarrhea during the R-CDI. Error bars indicate the mean ± S.E.M. Statistical analysis was performed by **a**−**c,** Student's *t*-test, **g**−**j**; Mann-Whitney test; **l**, Kruskal- Wallis, post-Dunn's; **m**, **n**, Wilcoxon matched-pairs signed-rank test; **o**, Log-rank (Mantel-Cox) test; ns indicates non-significant differences, * $P < 0.05$, ** $P < 0.001$.

Extended Data Figure Legends

Extended Data Fig. 1 | Adherence of *C. difficile* spores to the colonic mucosa. *z*-plane and orthogonal view of confocal micrographs of fixed whole-mount colonic tissue of mice. Panels **a**−**c**, **g** micrographs of colon of C57BL/6 mice infected in a colonic loop model with 5×10^8 *C. difficile* R20291 spores for 5 h. *C. difficile* spores are shown in red, F-actin is shown in green and nuclei in blue (fluorophores colors were digitally reassigned for a better representation). Panels **d**−**f**, **h** are a magnification of panels **a**−**c**, **g** respectively. Highlighted are *C. difficile* spores close the apical membrane of cells. Micrographs are representative of 3 independent mice. Bars **a**−**c**, **g** 50 μm, **d**−**f**, **h** 10 μm.

Extended Data Fig. 2 | Adherence of *C. difficile* spores to the intestinal mucosa. *z*-plane and orthogonal view of confocal micrographs of fixed whole-mount colonic tissue of mice. Panels **a**−**c**, **g** micrographs of ileum mucosa of C57BL/6 mice infected in an ileal loop model with 5×10^8 spores *C. difficile* R20291 spores for 5 h. *C. difficile* spores are shown in red, F-actin is shown in green and nuclei in blue (fluorophores colors were digitally reassigned for a better representation). Panels **d**−**f**, **h** are a magnification of panels **a**−**c**, **g** respectively. Highlighted are *C. difficile* spores close the apical membrane of cells. Micrographs are representative of 3 independent mice. Bars **a**−**c**, **g**, 50 μm, **d**−**f**, **h**, 10 μm.

Extended Data Fig. 3 | Internalization of *C. difficile* spores to the colonic mucosa *in vivo*. *z*-plane and orthogonal view of confocal micrographs of fixed whole-mount colonic tissue of mice. Panels **a**−**c**, **g**, Confocal micrographs of the colonic mucosa of C57BL/6

mice infected in a colonic loop model with 5×10^8 *C. difficile* R20291 spores for 5 h. *C. difficile* spores are shown in red, F-actin is shown in green and nuclei in blue (fluorophores colors were digitally reassigned for a better representation). Panels **d**−**f**, **h** are a magnification of panels **a**−**c**, **g**, respectively. Highlighted are *C. difficile* spores close the apical membrane of cells. Micrographs are representative of 3 independent mice. Bars **a**−**c**, **g**, 50 μm, **d**−**f**, **h**, 10 μm.

Extended Data Fig. 4 | Internalization of *C. difficile* spores into the intestinal mucosa. *z*-plane and orthogonal view of confocal micrographs of fixed whole-mount colonic tissue of mice. Panels **a**−**c** micrographs of the ileum mucosa of C57BL/6 mice infected in an ileal loop model with 5×10^8 spores *C. difficile* R20291 spores for 5 h. *C. difficile* spores are shown in red, F-actin is shown in green and nuclei in blue (fluorophores colors were digitally reassigned for a better representation). Panels **d**−**f**, **h** are magnification of panels **a**−**c**, **g** respectively. Highlighted are *C. difficile* spores close the apical membrane of cells. Micrographs are representative of 3 independent mice. Bars **a**−**c**, **g** 50 μm, **d**−**f**, **h** 10 μm.

Extended Data Fig. 5 | Distribution of internalized *C. difficile* spore in colonic and in ileum mucosa. a Schematics of the method applied for measurements of distances of internalized spores in the ileum mucosa. Distribution of the distance of internalized *C. difficile* spores to the **b** villus tip or to **c** the villus membrane. **d** Schematics of the method applied for measurements of distances of internalized spores in the colonic mucosa. **e** Distribution of the distance of internalized *C. difficile* spores to the colonic epithelium surface or **f** to the closest crypt axis. In the ileum, distance from 34 internalized *C. difficile*

spores to the villus tip and the distance of 54 internalized *C. difficile* spores to the villus membrane is shown. In the colon, the distance of 61 internalized *C. difficile* spores was evaluated.

Extended Data Fig. 6 | Confocal microscopy of internalized *C. difficile* spores into intestinal epithelial cells *in vitro*. *z*-plane and orthogonal view of confocal micrographs of **a**, **b** polarized T84 cells infected with NHS-treated R20291 spores for 5 h. **c**, **d** Intestinal epithelial Caco-2 cells infected with NHS-treated *C. difficile* R20291 spores. *C. difficile* spores are shown in red, F-actin is shown in green, (fluorophores colors were digitally reassigned for a better representation). Scale bar, 10 µm.

Extended Data Fig. 7 | Internalized spores are not stained with anti-*C. difficile* spore goat serum in non-permeabilized cells, and serum increases the internalization into Caco-2 cells. **a**, Cells were infected for 3 h with FBS treated *C. difficile* R20291 spores, and without permeabilization, spores were immunodetected as is described in methods. Bright spores that were not detected with fluorescent-labeled antibodies were considered as internalized. Dynamic of *C. difficile* spore-entry of spores pre-incubated with FBS in infected **i** Caco-2, and **j** T84 cells for 3h in the presence of 10% FBS. **k** Internalization of *C. difficile* spores of clinical isolates of various ribotypes into Caco-2 cells. Error bars indicate the mean ± S.E.M. Statistical analysis was performed by Student's *t*-test. ns, indicates non-significant differences, $*P < 0.01$.

Extended Data Fig. 8 | The spore entry into Caco-2 cell line in the presence of normal

human serum is inhibited by RGD peptide. a−b Caco-2 cells monolayer differentiated, and **c–f** undifferentiated. **a**, **c**, **e** show relative internalization while **b**, **d**, **f** shows relative adherence compared to the control (0 μg mL^{-1} RGD). Before the infection, spores were incubated with **a**, **b**, **e**, **f** culture media; **c**, **d** with NHS. Cells were incubated with 0 and 5 μg mL^{-1} of RGD peptide and infected with R20291 *C. difficile* spores pre-incubated with DMEM (without serum) or NHS. The data represents the mean of three biological experiments. Error bars indicate the mean ± S.E.M. Statistical analysis was performed by Student's *t*-test, ns, indicates non-significant differences, **P* < 0.0001.

Extended Data Fig. 9 | *C. difficile* spore entry of *C. difficile* spore pre-incubated Fn and Vn and Caco-2 cells pre-incubated Fn and Vn. a−d Caco-2 cells monolayers undifferentiated and **e**, **f** 8 days differentiated. **a**, **c**, **e** shows relative internalization, while **b** **d**, **f** shows relative adherence compared to the control (DMEM). Before infecting cells, **a, b** spores or **c, d** Caco-2 cells were pre-treated with NHS, Fn or Vn, and subsequently infected with *C. difficile* R20291 spores. The data represents the mean of three biological experiments. Error bars indicate the mean ± S.E.M. Statistical analysis was performed by Student's *t*-test, ns indicates non-significant differences **P* < 0.005; ***P* < 0.001.

Extended Data Fig. 10 | Accessibility Muc2 in the small intestine. a Confocal micrographs of fixed whole-mounted healthy colon of C57BL/6 mice for acc Muc2 with acc Ecad. The main figure shown a 3D projection, below magnifications and a z-stack of representative cells with the different immunostaining. **b** Shown the cell repartition of cells immunodetected for acc Ecad. **c** Cell repartition of cells immunodetected for Muc2. **d** Cell

repartition of total acc Muc2 cells that were immunodetected for acc E-cad. Acc-Muc2 is shown in green Acc Ecad is shown in red and F-actin in grey (fluorophores colors were digitally reassigned for a better representation). Scale bar, 20µm, in magnifications 10µm. Micrographs are representative of mice (n = 2). 1,000 - 1,200 cells were counted for each mouse in an area 84,628µm^2. Error bars indicate mean ± S.E.M.

Extended Data Fig. 11 | The spore entry into Caco-2 cells mediated by Fn occurs through integrin subunits α_5 and β_1; while internalization mediated Vn is through integrin subunits α_v and β_1. a–f undifferentiated and **g**, **h** differentiated Caco-2 cell monolayer, and were pre-incubated with **a**–**d** 1, 3 or 5 µg mL^{-1} of RGD peptide or **e**–**h** 10 µg mL^{-1} of antibody against α_v, α_2, α_5, β_1, β_3, non-immune IgG antibody in DMEM and infected with *C. difficile* R20291 spores pre-incubated with 10 µg mL^{-1} **a**, **b, e, f** Fn, or **c**, **d, g, h** Vn. **a**, **c**, **e**, **g** Show relative internalization while **b**, **d**, **f**, **h** relative adherence compared to the control (no RGD or non-immune IgG antibody). Error bars indicate the mean ± S.E.M. Statistical analysis was performed by Student's *t*-test, ns indicates non-significant differences, $P < 0.01$, $^{**}P < 0.001$.

Extended Data Fig. 12 | Serum-free medium does not promote internalization of *C. difficile* spores dependent of integrins α_v, α_5, and β_1. a Internalization or **b** adherence of *C. difficile* pre-treated 1 h with DMEM in CHO cells ectopically expressing α_v, α_5, β_1 integrins relative to the control (wild-type CHO cells). Error bars indicate the mean ± S.E.M. Statistical analysis was performed by Student's *t*-test, ns indicates non-significant differences, $P < 0.01$, $^{**}P < 0.001$.

Extended Data Fig. 13 | Quantification of *C. difficile* spores associated with Fn and Vn by TEM. **a**, **b**, percentage of the total of labeled spores treated with Fn or Vn (Fn + or Vn + respectively) and the negative control without protein (Fn - or Vn - as appropriate). Error bars indicate the mean ± S.E.M. Statistical analysis was performed by Student's *t*-test, ns indicates non-significant differences, *$P < 0.001$.

Extended Data Fig. 14 | Deletion of *bclA3* genes in R20291. The deletion of *bclA3* was done by allelic exchange through a schematic representation of the deletion of *bclA3*, leaving a small peptide in frame. Construction and characterization of *bclA3* mutant in *C. difficile*. **a** Schematic representation of in-frame deletion of *bclA3*. **b** The size of *bclA3* loci was verified by PCR using detection primers (Table S2).

Extended Data Fig. 15 | Immunofluorescence intensity of the anti-spore in *bclA3* mutant

***C. difficile* spores. a** Wild-type (Δ*pyrE*/*pyrE*$^+$), Δ*bclA3* and Δ*bclA3*/*bclA3*$^+$ R20291 spores are recognized by anti-*C. difficile* spore goat serum. Δ*pyrE/pyrE*$^+$, (wild-type; wt), Δ*bclA3*, and complemented mutant (*ΔbclA3/bclA3*$^+$) R20291 spores were fixed on glass coverslips treated with poly-lysine; then the samples were blocked with PBS–1% BSA and were labeled for 1 h with goat-anti-spore serum and incubated with secondary antibody anti-goat CFL 488-conjugated; then, micrograph were captured with epifluorescence microscopy. **b** Quantitative analysis of the fluorescence (Fl.) intensity in spores of Δ*pyrE/pyrE*$^+$ (dark line), Δ*bclA3* (red line) and Δ*bclA3/bclA3*$^+$ (blue line), the values shown in the graphs the

normalized fluorescence intensity from 150 spores of Δ*pyrE/pyrE*$^{+}$, Δ*bclA3* and Δ*bclA3/bclA3*$^{+}$ strain. **c** Distribution of the fluorescence intensity of wild-type (dark bars), Δ*bclA3* (red bars) and Δ*bclA3/bclA3*$^{+}$ (blue bars) spores.

Extended Data Fig. 16 | Effect of absence of BclA3 on spore-entry and adherence to non-phagocytic cells. Relative *C. difficile* spore **a**, **c** internalization and **b**, **d** adherence of HeLa cells infected with *C. difficile* spores Δ*pyrE/pyrE*$^{+}$ (wild-type), Δ*bclA3*, and Δ*bclA3/bclA3*$^{+}$ pre-incubated with 10 µg of **a**, **b** Fn or **c**, **d** Vn. **e**−**h** shown the relative *C. difficile* spore adherence of CHO cells ectopically expressing integrins; **e**, CHO-α_5, **f**, **h** CHO-β_1 and **g** CHO-α_v and infected with *C. difficile* spores Δ*pyrE/ pyrE*$^{+}$ (wild-type), Δ*bclA3*, and Δ*bclA3/bclA3*$^{+}$ pre-incubated with 10 µg of **e**, **f** Fn or **g**, **h** Vn. The data represents the mean of three biological experiments. Error bars indicate the mean ± S.E.M. Statistical analysis was performed by Student's *t*-test, ns indicates non-significant differences, $*P < 0.001$.

Extended Data Fig. 17 | Representative confocal micrograph of adhered and internalized *C. difficile* spores in colonic mucosa with Δ*bclA3* spores and Extended data of BclA exosporium protein contributes to the recurrence of *C. difficile* infection. There are supplementary figures of the experiment detailed in Fig 6. Confocal micrograph of the whole-mount fixed colon. C57BL/6 mice infected in a colonic loop model with 5×10^8 *C. difficile* R20291 spores. Panels shown confocal micrographs of adhered and internalized spores in colon loop infected with strains **a** wild-type (Δ*pyrE*/*pyrE*$^{+}$), **b**

Δ*bclA3*, and **c** Δ*bclA3*/*bclA3*$^{+}$. The main figure shown a 3D projection, below the z-stack, magnification, and the orthogonal view. *C. difficile* spores are shown in red, F-actin is shown in green and nuclei in blue (fluorophores colors were digitally reassigned for a better representation). The white arrow indicates internalized *C. difficile* spores, empty arrow indicates adhered *C. difficile* spore. Micrograph are representative of mice wild type (n = 10); Δ*bclA3* (n = 12) and Δ*pyrE*/*pyrE*$^{+}$ (n = 11). These are supplementary figures from the experiment of R-CDI in animals infected with Δ*bclA3* spores (Fig. 6). Animals were infected with wild-type (Δ*pyrE*/*pyrE*$^{+}$; n = 10), Δ*bclA3* (n = 16) and Δ*bclA3*/*bclA3*$^{+}$, (n = 14) and were monitored daily for **d** relative weight; **e** time to diarrhea during CDI. **f** *C. difficile* spore CFU in feces during CDI and R-CDI. Spore adherence to the colonic tract was evaluated on day 11 to **g** Cecum, **h** proximal colon, **i** distal colon and, **j** cytotoxicity of the cecal content. Error bars indicate the mean ± S.E.M. Statistical analysis was performed by **d**, **f,** Kruskal- Wallis, post-Dunn's test, **e,** Log-rank (Mantel-Cox), **g**−**j,** Mann-Whitney test, ns indicates non-significant differences, * $P < 0.05$, ** $P < 0.01$, ***P < 0.001. Scare bar, 20μm.

Extended Data Fig. 18 | Extended data of Fig 7. These are supplementary figures from the experiment detailed in Fig 7. *C. difficile* spore **a** internalization and **b** adherence in monolayers of T84; cells were pre-treated with 30 μM of nystatin (shown as NYS) for 1 h and were subsequently infected with *C. difficile* spores R20291 pre-treated for 1 h with FBS. **c** Cellular viability after nystatin treatment was determined by using MTT assay. **d–f** Confocal micrograph of the whole-mount fixed colon. C57BL/6 mice infected in a colonic loop model with 5×10^{8} *C. difficile* R20291spores. Panels shown adhered and internalized

spores of **d** untreated mice (Ctrl), **e** mice treated 24h before the surgery with nystatin, and administered in the loop in the presence of: **f** 250 nmol of RGD peptide in the loop. The main figure shown a 3D projection, below the z-stack, magnification, and the orthogonal view. *C. difficile* spores are shown in red, F-actin is shown in green and nuclei in blue (fluorophores colors were digitally reassigned for a better representation). White arrow indicates internalized *C. difficile* spores, empty arrow indicates adhered *C. difficile* spore. Micrographs are representative of mice (n = 4). These are supplementary figures from the experiment of R-CDI with animals treated with nystatin and RGD. Animals were infected with *C. difficile* R20291 and were monitored daily for **g** weight loss, **h** diarrhea, and **i** *C. difficile* spore CFU in feces during CDI and R-CDI. For mice treated with nystatin and vancomycin (n = 18) or vancomycin alone as control (n = 23) from days 3-7. Vancomycin is shown as VAN. Error bars indicate the mean ± S.E.M. Statistical analysis was performed by **a, b,** Student's *t*-test, **f** and **h,** Kruskal-Wallis, post-Dunn's test, **g**, Log-rank (Mantel-Cox), ns indicates non-significant differences, *P < 0.05, **P < 0.01, ***P < 0.001. Scale bar, 20µm.

Supplementary Videos

Video 1. Wild-type *C. difficile* spores internalize in colonic mucosa.

Travel through a confocal *Z*-stack from the apical face of the colonic mucosa. *C. difficile* spore is shown in red, F-actin is shown in green and nuclei in blue (fluorophores colors were digitally reassigned for a better representation). Arrows indicate internalized spores.

Video 2. Wild-type *C. difficile* spores internalize in the ileum mucosa.

Travel through a confocal *Z*-stack from the apical face of the ileum mucosa. *C. difficile* spore is shown in red, F-actin is shown in green and nuclei in blue (fluorophores colors were digitally reassigned for a better representation). Arrows indicate internalized spores.

Figure 1

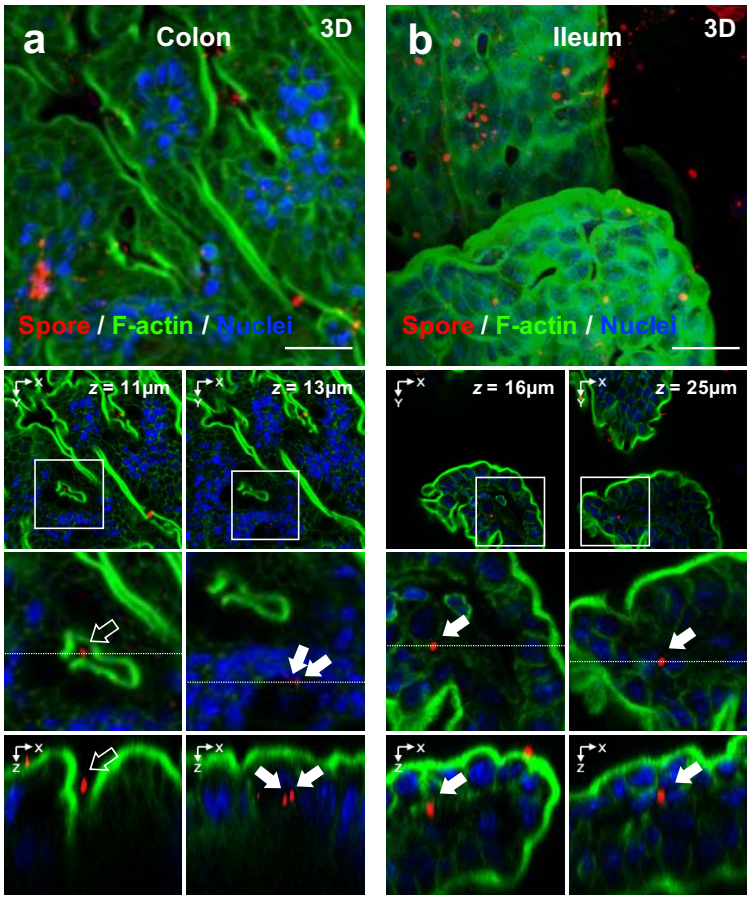
a
Colon
3D
Spore / F-actin / Nuclei
b
Ileum
3D
Spore / F-actin / Nuclei
z = 11µm
z = 13µm
z = 16µm
z = 25µm

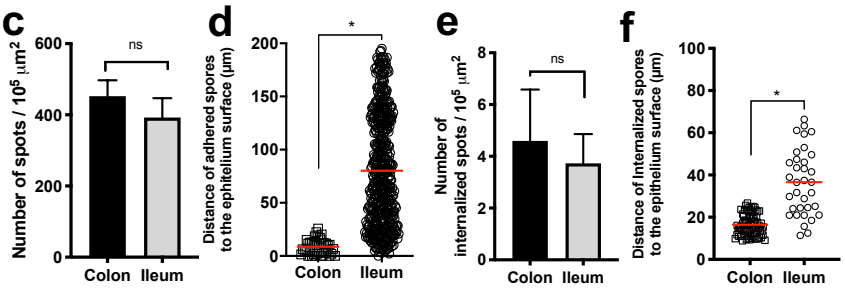
c
Number of spots / 10⁵ µm²
ns
Colon
Ileum
d
Distance of adhered spores to the ephitelium surface (µm)
*
Colon
Ileum
e
Number of internalized spots / 10⁵ µm²
ns
Colon
Ileum
f
Distance of internalized spores to the epithelium surface (µm)
*
Colon
Ileum

Figure 2

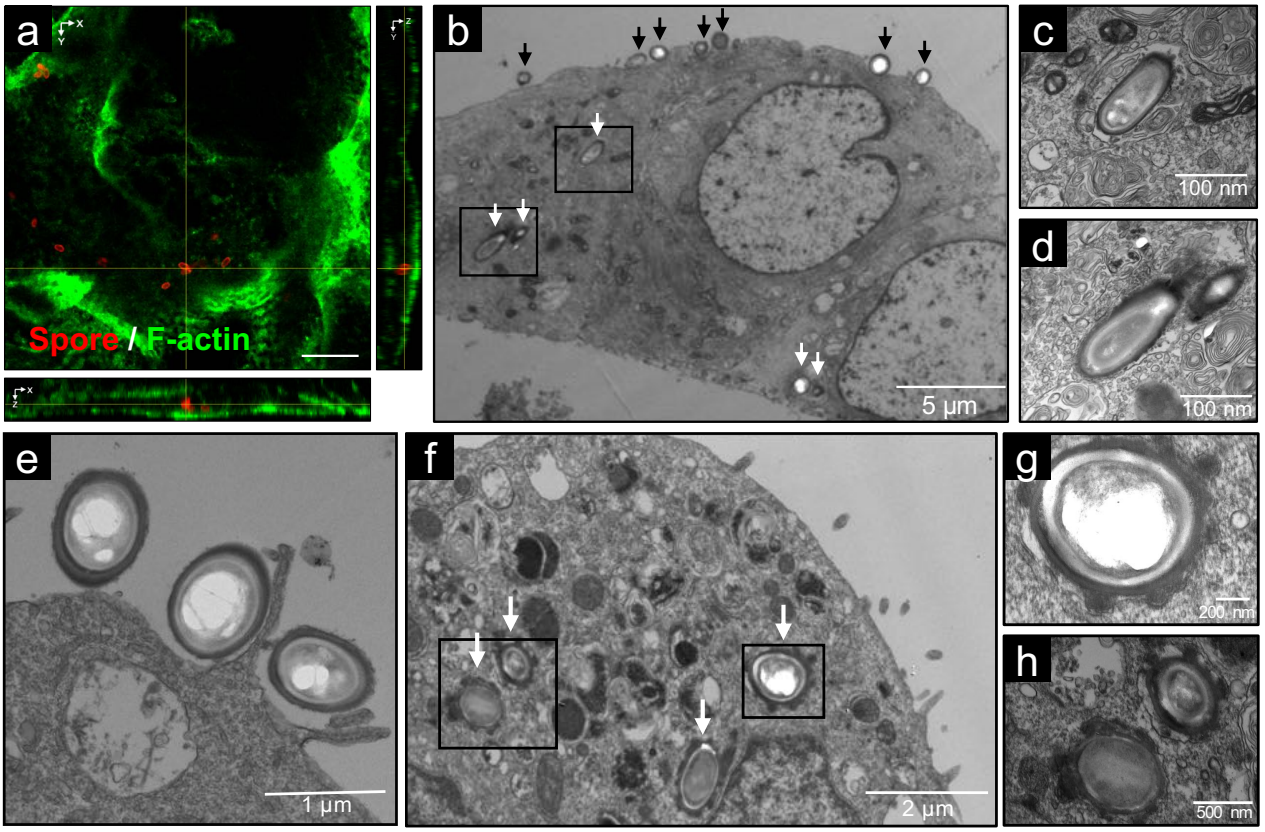
a
Spore / F-actin
b
5 µm
c
100 nm
d
100 nm
e
1 µm
f
2 µm
g
200 nm
h
500 nm

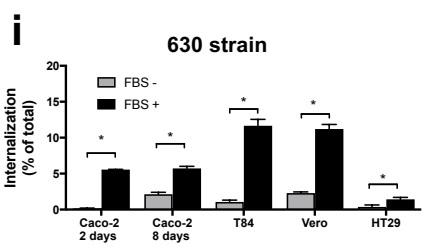
i
630 strain
Internalization (% of total)
FBS -
FBS +
Caco-2 2 days
Caco-2 8 days
T84
Vero
HT29

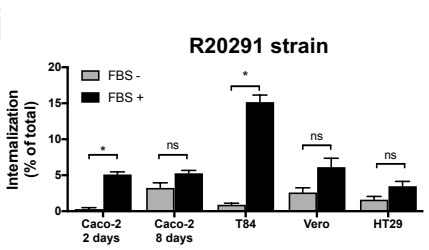
j
R20291 strain
Internalization (% of total)
FBS -
FBS +
ns
Caco-2 2 days
Caco-2 8 days
T84
Vero
HT29

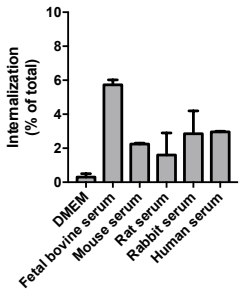
k
Internalization (% of total)
DMEM
Fetal bovine serum
Mouse serum
Rat serum
Rabbit serum
Human serum

Figure 3

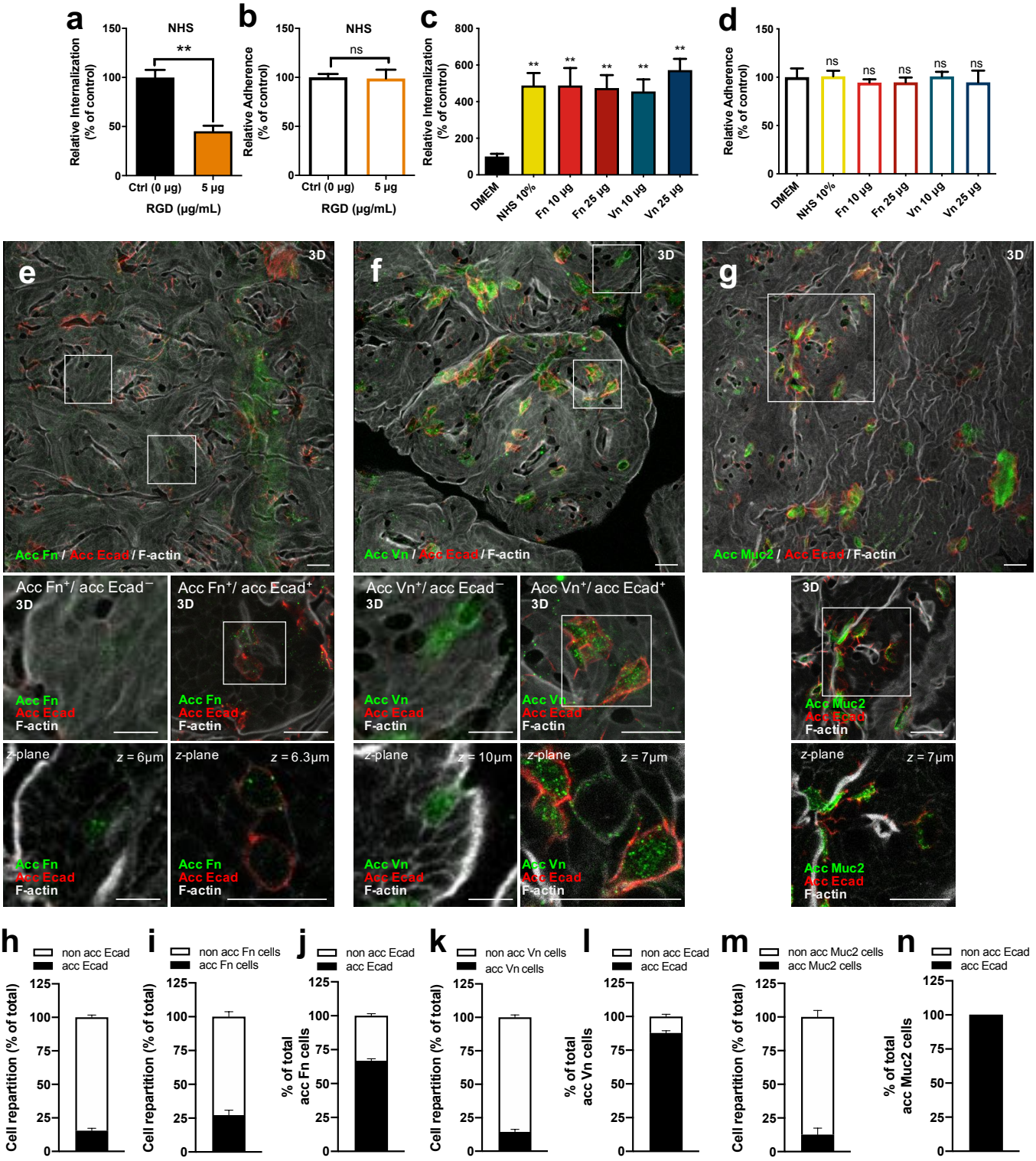
a
NHS
Relative Internalization (% of control)
150
100
50
0
**
Ctrl (0 µg)
5 µg
RGD (µg/mL)
b
NHS
Relative Adherence (% of control)
ns
c
Relative Internalization (% of control)
800
600
400
200
DMEM
NHS 10%
Fn 10 µg
Fn 25 µg
Vn 10 µg
Vn 25 µg
d
Relative Adherence (% of control)
ns
e
3D
Acc Fn / Acc Ecad / F-actin
f
Acc Vn / Acc Ecad / F-actin
g
Acc Muc2 / Acc Ecad / F-actin
Acc Fn+/ acc Ecad−
Acc Fn+/ acc Ecad+
Acc Vn+/ acc Ecad−
Acc Vn+/ acc Ecad+
Acc Fn
Acc Ecad
Acc Vn
Acc Muc2
F-actin
z-plane
z = 6µm
z = 6.3µm
z = 10µm
z = 7µm
h
non acc Ecad
acc Ecad
Cell repartition (% of total)
i
non acc Fn cells
acc Fn cells
j
% of total acc Fn cells
k
non acc Vn cells
acc Vn cells
l
% of total acc Vn cells
m
non acc Muc2 cells
acc Muc2 cells
n
% of total acc Muc2 cells

Figure 4

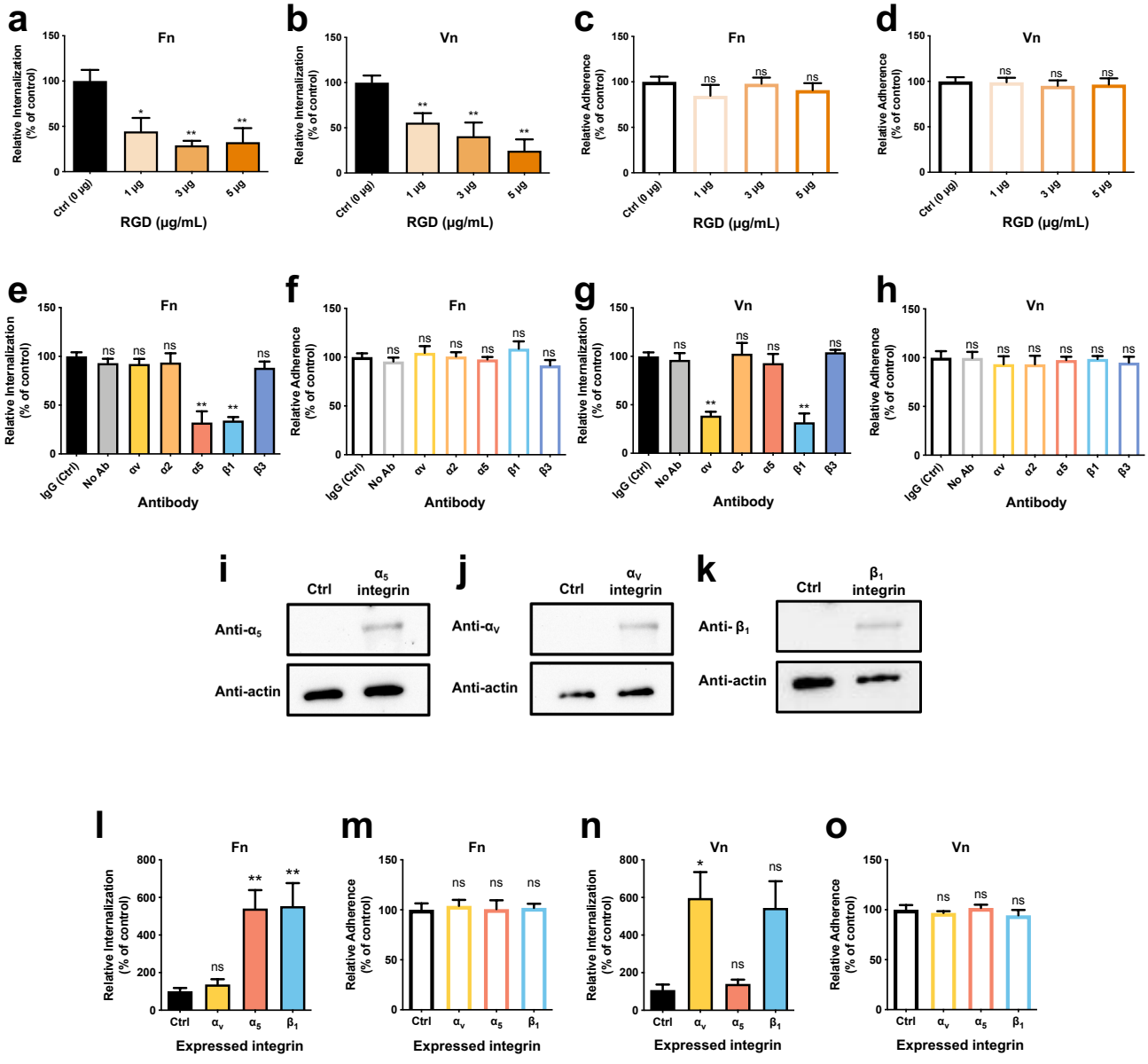
a
Fn
Relative Internalization (% of control)
RGD (μg/mL)
b
Vn
c
Fn
Relative Adherence (% of control)
d
Vn
e
Fn
Antibody
f
Fn
g
Vn
h
Vn
IgG (Ctrl)
No Ab
αv
α2
α5
β1
β3
i
Ctrl
α5 integrin
Anti-α5
Anti-actin
j
αV integrin
Anti-αV
k
β1 integrin
Anti- β1
l
Fn
Expressed integrin
m
Fn
n
Vn
o
Vn

Figure 5

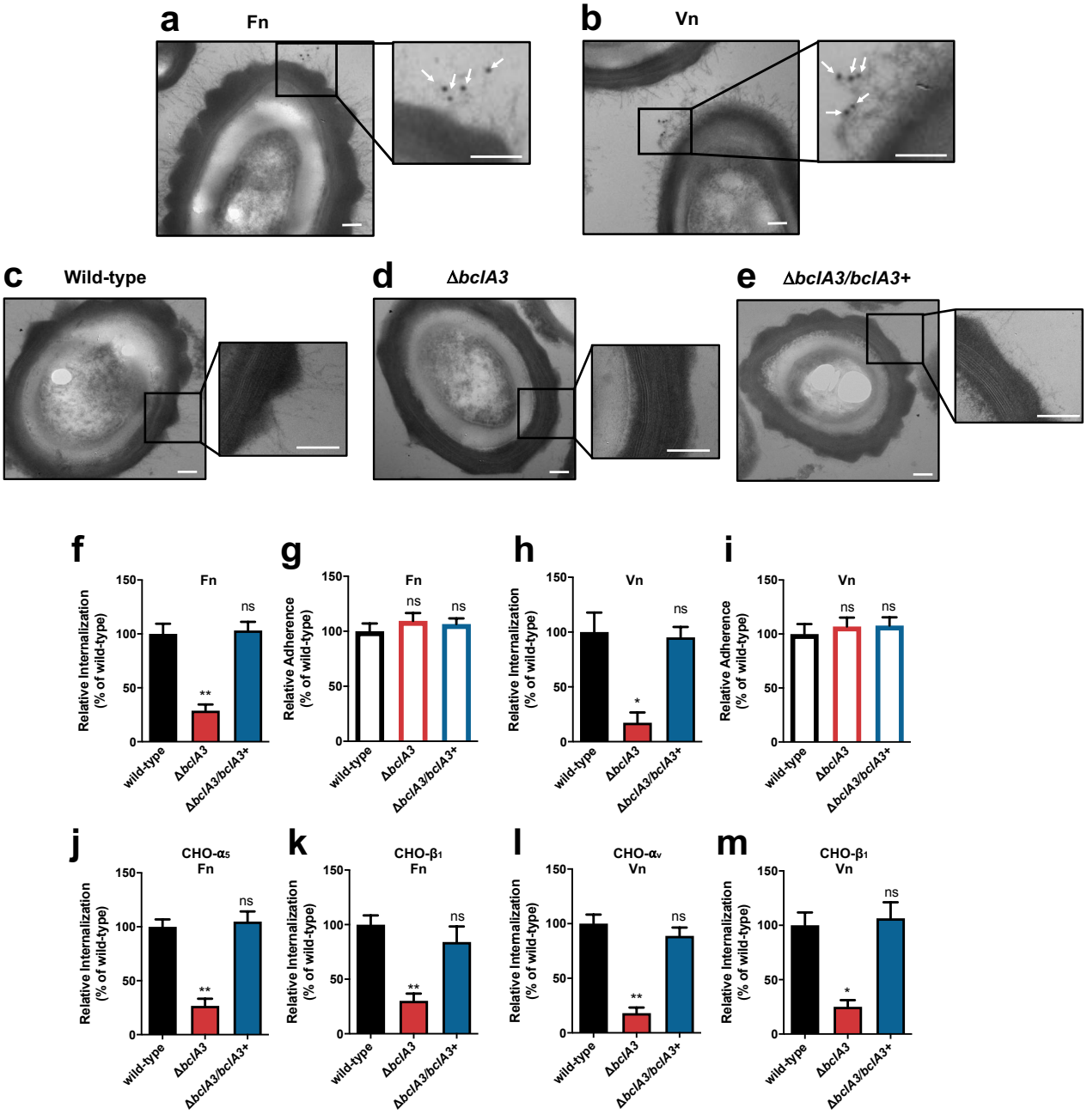
a
Fn
b
Vn
c
Wild-type
d
ΔbclA3
e
ΔbclA3/bclA3+
f
Fn
Relative Internalization (% of wild-type)
g
Fn
Relative Adherence (% of wild-type)
h
Vn
Relative Internalization (% of wild-type)
i
Vn
Relative Adherence (% of wild-type)
j
CHO-α5
Fn
Relative Internalization (% of wild-type)
k
CHO-β1
Fn
Relative Internalization (% of wild-type)
l
CHO-αv
Vn
Relative Internalization (% of wild-type)
m
CHO-β1
Vn
Relative Internalization (% of wild-type)
150
100
50
0
ns
**
*
wild-type
ΔbclA3
ΔbclA3/bclA3+

Figure 6

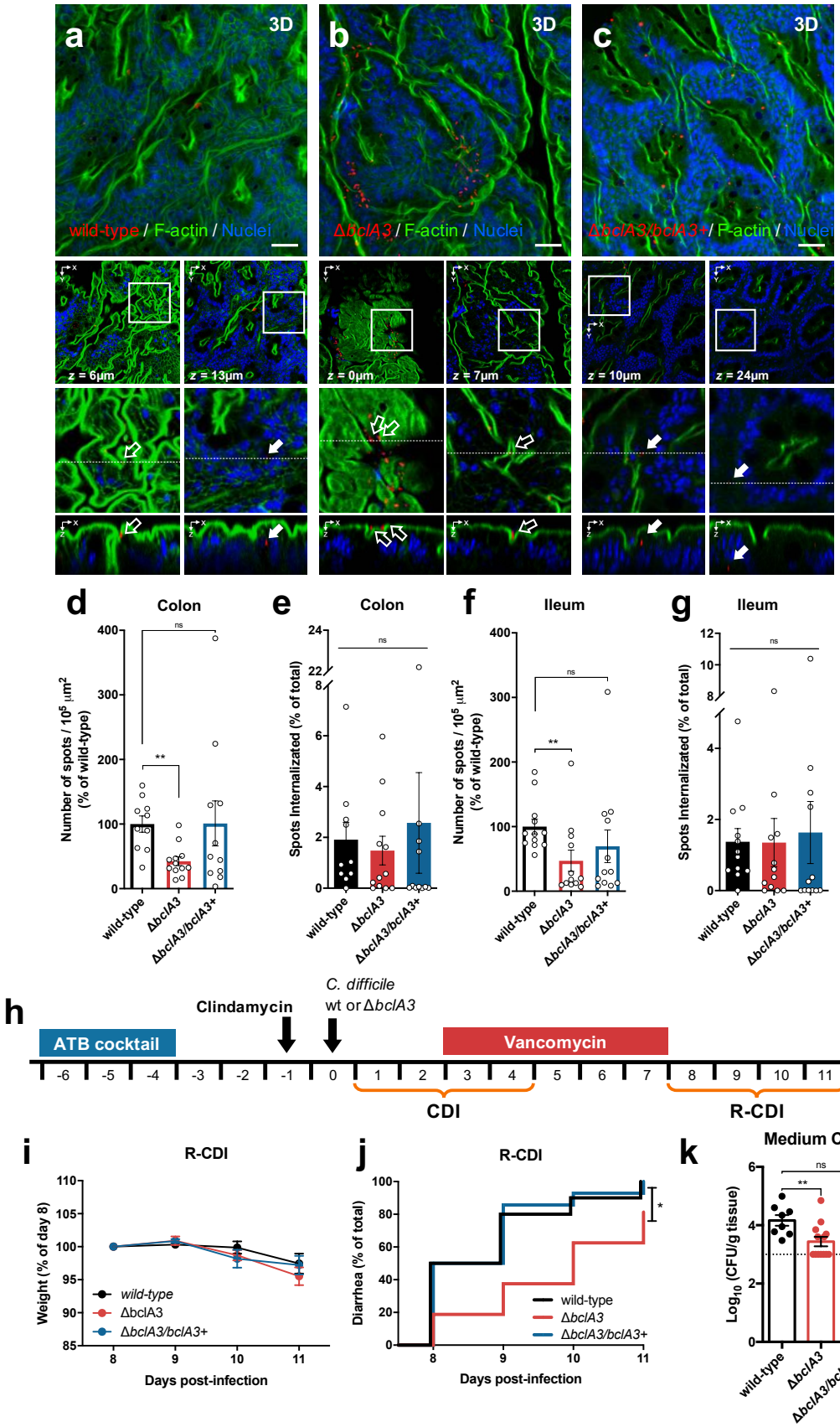
a
3D
wild-type / F-actin / Nuclei
b
3D
ΔbclA3 / F-actin / Nuclei
c
3D
ΔbclA3/bclA3+ / F-actin / Nuclei
z = 6µm
z = 13µm
z = 0µm
z = 7µm
z = 10µm
z = 24µm
d
Colon
Number of spots / 10^5 µm^2 (% of wild-type)
ns
**
wild-type
ΔbclA3
ΔbclA3/bclA3+
e
Colon
Spots Internalizated (% of total)
f
Ileum
Number of spots / 10^5 µm^2 (% of wild-type)
g
Ileum
Spots Internalizated (% of total)
h
Clindamycin
C. difficile
wt or ΔbclA3
ATB cocktail
Vancomycin
-6 -5 -4 -3 -2 -1 0 1 2 3 4 5 6 7 8 9 10 11
CDI
R-CDI
i
R-CDI
Weight (% of day 8)
wild-type
ΔbclA3
ΔbclA3/bclA3+
Days post-infection
j
R-CDI
Diarrhea (% of total)
*
wild-type
ΔbclA3
ΔbclA3/bclA3+
Days post-infection
k
Medium Colon
Log10 (CFU/g tissue)
ns
**
wild-type
ΔbclA3
ΔbclA3/bclA3+

Figure 7

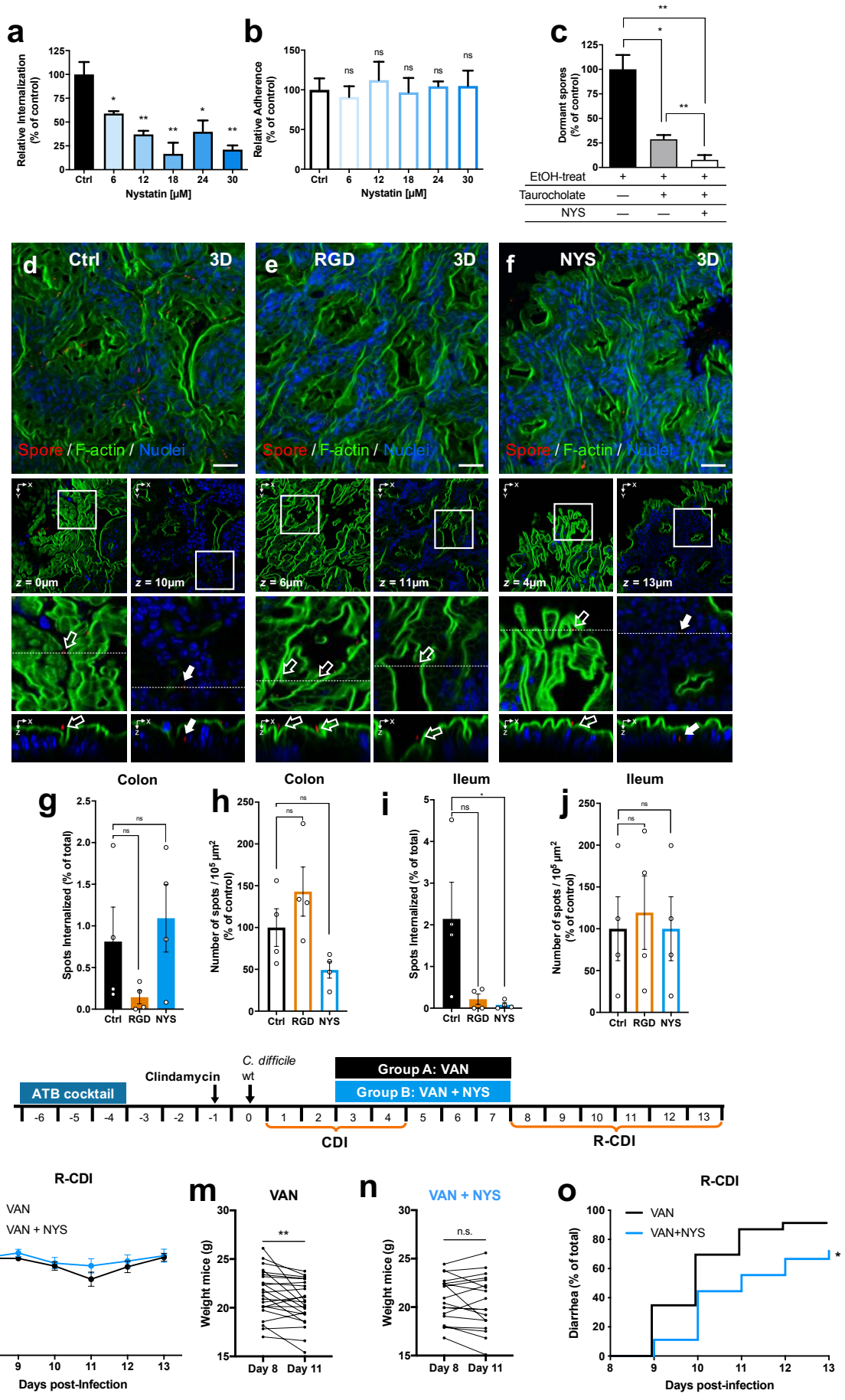
a
Relative Internalization (% of control)
Nystatin [µM]
Ctrl
6
12
18
24
30
b
Relative Adherence (% of control)
ns
c
Dormant spores (% of control)
EtOH-treat
Taurocholate
NYS
d Ctrl 3D
e RGD 3D
f NYS 3D
Spore / F-actin / Nuclei
z = 0µm
z = 10µm
z = 6µm
z = 11µm
z = 4µm
z = 13µm
g Colon
Spots Internalized (% of total)
h Colon
Number of spots / 10⁵ µm² (% of control)
i Ileum
Spots Internalized (% of total)
j Ileum
Number of spots / 10⁵ µm² (% of control)
k
ATB cocktail
Clindamycin
C. difficile
wt
Group A: VAN
Group B: VAN + NYS
CDI
R-CDI
l R-CDI
Weight (% of day 8)
VAN
VAN + NYS
Days post-Infection
m VAN
Weight mice (g)
Day 8
Day 11
n VAN + NYS
n.s.
o R-CDI
Diarrhea (% of total)
VAN+NYS
Days post-infection